

LIBRARY Michigan State University

This is to certify that the

thesis entitled

PETROCHEMISTRY OF THE QUINN CANYON SILICIC INTRUSIVES, NYE COUNTY, NEVADA: A COMPARISON WITH CLIMAX-TYPE PORPHYRY MO SYSTEMS

presented by

James S. Guentert

has been accepted towards fulfillment of the requirements for

Masters degree in Geology

Major professor

Date_5/19/88

g 4 ...



RETURNING MATERIALS:
Place in book drop to remove this checkout from your record. FINES will be charged if book is returned after the date stamped below.

PETROCHEMISTRY OF THE QUINN CANYON SILICIC INTRUSIVES, NYE COUNTY, NEVADA: A COMPARISON WITH CLIMAX-TYPE PORPHYRY Mo SYSTEMS

Ву

James S. Guentert

A THESIS

Submitted to
Michigan State University
in partial fulfillment of the requirements
for the degree of

MASTER OF SCIENCE

Department of Geological Sciences

1988

ABSTRACT

PETROCHEMISTRY OF THE QUINN CANYON SILICIC INTRUSIVES, NYE COUNTY, NEVADA: A COMPARISON WITH CLIMAX-TYPE PORPHYRY Mo SYSTEMS

Ву

James S. Guentert

The Quinn Canyon Range (QC) has anomalous concentrations of Mo, W, Sn, Pb and fluorite mineralization associated with the emplacement of 23 m.y. high silica rhyolite intrusives. This investigation focuses on the comparison of QC dikes and plugs with the rhyolitic compositions associated with porphyry Mo, W, Sn, and lithophile element metallization.

The most evolved QC rhyolites have lower Rb, Th, and Nb, higher Ba and Sr and smaller La/YbN ratios than the granitoids at Climax, Urad-Henderson and Mt. Emmons (except Rb). The QC rhyolites are chemically more similar to the rhyolites generating Mo mineralization at Pine Grove, Utah. Based on the elements analyzed (no F or Cl) the QC rhyolites seem to qualify as topaz rhyolites.

Because of general similarities with Pine Grove, the possiblity of Mo mineralization at Quinn Canyon cannot be discounted at this stage of study. Differences in trace element chemistry and source material with Climax and Urad-Henderson granitoids suggest that any Mo mineralization probably would be uneconomic.

ACKNOWLEDGEMENTS

I would like to thank my advisor, John Wilband for all his help, encouragement, and advise during the preparation of this thesis. His willingness to take the time (even on weekends) to answer questions and assist me in any way is greatly appreciated. I am particularly indebted to him for his help in the field. I also would like to acknowledge the interest and assistance of committee members Dr. Tom Vogel and Dr. Bill Cambray.

Special thanks go to my good friend Dave Westjohn for suggesting this study, reviewing and critiquing the thesis and in general offering his encouragement and advise when necessary.

I would like to express my gratitude to the friends I have made during my tenure at MSU. Among these are: Don Jessup, Dave Cook, John Salvino, Steve Young, Bob Cuniff, Soo Meen Wee, Jim Mills, Jim Gell, Paul Carter and especially Bill Sack.

My most sincere and heartfelt thanks go to my wife and best friend Linda.

Amoco Minerals Co. supplied exploration geochemical data for this study. Financial support was provided through a Chevron Graduate Fellowship and field work award and an MSU Teaching Assistantship.

TABLE OF CONTENTS

LIST OF FIGURES
LIST OF TABLES
INTRODUCTION
Problem
Method
PREVIOUS WORK
FIELD WORK
GEOLOGY OF THE QUINN CANYON RANGE
Sedimentary rocks
Igneous rocks
Structure
Economic geology
PETROGRAPHY
Mineralogy and texture
Alteration
PETROCHEMISTRY
Major elements
Alteration
Trace elements
Fluorite

REGIONAL GEOLOGY
Lineaments
Cenozoic igneous activity in the western U.S 43
Tertiary metallization in the western U.S 45
CLIMAX-TYPE PORPHYRY MOLYBDENUM DEPOSITS
Geology
Mineralogy and alteration
Petrochemistry of granitic rocks
Origin of granitic rocks
DISCUSSION AND RESULTS
Quinn Canyon silicic rocks
Petrochemical comparisons
Source material comparisons: isotopic evidence 71
Economic potential of the Quinn Canyon Range 78
CONCLUSIONS
Future work
APPENDIX A. CHEMICAL ANALYSES
APPENDIX B. ANALYTICAL METHODS
APPENDIX C. LOCATION OF SAMPLES
LIST OF REFERENCES

LIST OF FIGURES

Figure 1. Generalized geologic map of the Quinn Canyon Range (modified from Stewart and Carlson, 1977). Numbered areas denote location of anomalous element suites discussed in text
Figure 2. The Blue Ribbon Lineament and other mineral belts of eastern Nevada and western Utah
Figure 3. Major element variation diagrams for the Quinn Canyon silicic rocks. Highly altered samples denoted by a \diamond See figure 5 for group symbols
Figure 4. Plots of Sr, Zr, and Eu vs SiO2 for the Quinn Canyon rocks. Highly altered samples denoted by a . See figure 5 for group symbols
Figure 5. Plots of La and Zr vs Y for the Quinn Canyon sample groups
Figure 6. Arthimetic mean of selected trace elements of the Quinn Canyon sample groups, normalized to U.S.G.S. standard RGM-1 (rhyolite)
Figure 7. Chondrite-normalized REE patterns for the rhyodacites and low silica rhyolites
Figure 8. Chondrite-normalized REE patterns for the rhyolites and incompatible element-rich rhyolites
Figure 9. Chondrite-normalized REE patterns for the muscovite-bearing rhyolites group 1 and 2
Figure 10. Plots of Mo and Sn vs Pb for the incompatible element-rich rhyolites. Analyses by Bondar and Clegg, Ltd39

Figure 11. Distribution of topaz rhyolites of the western U.S. relative to the location of the Quinn Canyon Range, the Pine Grove porphyry Mo system and the Urad-Henderson, Climax and Mt. Emmons porphyry Mo deposits of the Colorado Mineral Belt (COMB) 46
Figure 12. Plot of Rb/Y vs Rb indicating possible partial melting (solid lines) and fractional crystallization (dashed lines) trends for the Quinn Canyon silicic rocks57
Figure 13. Plot of molecular Al203 vs molecular Na20+K20+CaO for the incompatible element-rich rhyolites and muscovite bearing rhyolites (group 1). Sample QC-13 has not been included because of alteration affecting NaO
Figure 14. Plots of Ba and Eu vs Nb, La and Zr vs Rb, and La and Zr vs Y for the incompatible element-rich rhyolites and muscovite-bearing rhyolites (group 1) 60
Figure 15. Enrichment factor diagrams of the Quinn Canyon incompatible element-rich rhyolites normalized to the mean of selected trace elements of rhyolites and granites form: a) Pine Grove (PG; this study), b) Pine Grove (PG; Keith, 1982), c) Mt. Emmons (ME) and d) Urad-Henderson (UH). The ranges of values for the Quinn Canyon rhyolites are shown by vertical bars 67
Figure 16. Chondrite-normalized REE patterns for Mt. Emmons and Urad-Henderson samples
Figure 17. Chondrite-normalized REE patterns for rhyolites of Pine Grove (this study) and Pine Grove (Keith, 1982)
Figure 18. Range of values of selected trace elements for topaz rhyolites of the western U.S. compared to the Quinn Canyon incompatible element-rich rhyolites. All values normalized to U.S.G.S. standard RGM-1. Vertical bars represent ranges of concentrations for the Quinn Canyon incompatible element-rich rhyolites (after Christiansen et al., 1986)

Figure 19. Map illustrating the intrepreted western limit of Precambrian basement (line 1) and western limit of a granulite grade lower crust (line 2) (Farmer and Depaolo, 1983). Lead isotopic provinces from Zartman (1974) are defined by stipled bands and identified by Roman numerals. See text for further explanation (modified from Farmer and Depaolo, 1983)	. 74
Figure 20. Lead isotope data for Pine Grove (PG), Quinn Canyon (QC), Urad-Henderson (UH), Mount Emmons (ME) and	
Climax (CM). The lead growth curves are from Stacey and Kramer (1975). Data from Zartman (1974), Stacey et al., 1968 and Stein (1985) (after Stein, 1985)	75

LIST OF TABLES

Table 1. Petrography of the Quinn Canyon silicic rocks1	8
Table 2. Arthimetic mean of selected trace elements for the Quinn Canyon silicic rocks	9
Table 3. Arthimetic mean of selected trace elements for the Climax-type rhyolites and the Quinn Canyon incompatible element-rich rhyolites	4
Table 4. Chemical analyses of the Quinn Canyon silicic rocks	3
Table 5. Chemical analyses of fluorite, highly altered samples and other samples from Quinn Canyon	7
Table 6. Commercial analyses done by Bondar and Clegg, Ltd	8
Table 7. Chemical analyses of rhyolites and granites from Mt. Emmons, Urad-Henderson, and Pine Grove 8	9
Table 8. Precision and accuracy	2

INTRODUCTION

Problem

The Quinn Canyon Volcanic complex of southeast central Nevada consists of Tertiary eruptive sequences, flows and hypabyssal dikes, plugs and sills, which overlie and intrude Paleozoic sedimentary rocks (Sainsbury and Kleinhampl, 1969). This mineralized volcanic center lies along the trend of the Pioche belt and the Blue Ribbon Lineament as defined by Shaw and Stewart (1976) and Rowly et al. (1978), a mineral belt characterized by the occurrence of fluorine, tungsten, gold, copper, molybdenum, lead-zinc-silver, manganese, uranium and berylium minerals (Figures 1 and 2).

The most evolved Quinn Canyon rhyolites are part of a chemically distinct group of high silica, fluorine-rich rhyolites located in the western United States. Typically, the hypabyssal intrusive and flow rocks are 10-30 m.y. old and their emplacement history generally coincides with late Cenozoic extensional faulting, and the onset of transitional to bimodal magmatism marking the end of Cenozoic subduction (Christiansen and Lipman, 1972; Lipman et al., 1976; Westra and Keith, 1981; Christiansen et al., 1983).

High silica, fluorine-rich rhyolites are frequently associated with epithermal base and precious metal veins (Ag, Au, Pb, Sn, W), fluorite-rich replacement and fracture

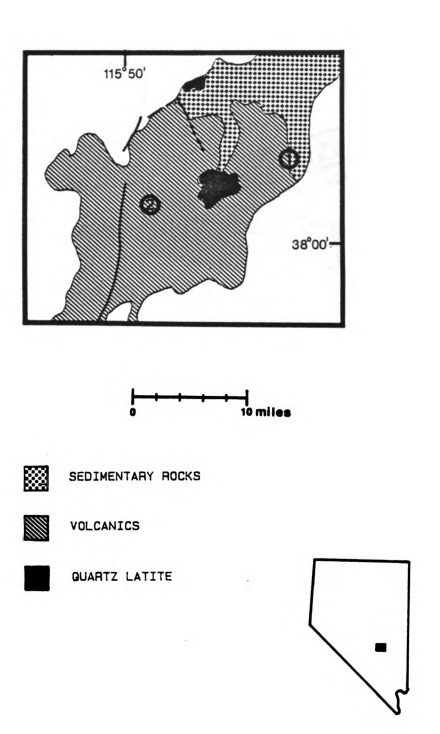


Figure 1. Generalized geologic map of the Quinn Canyon Range (modified from Stewart and Carlson, 1977). Numbered areas denote location of anomalous element suites discussed in text.

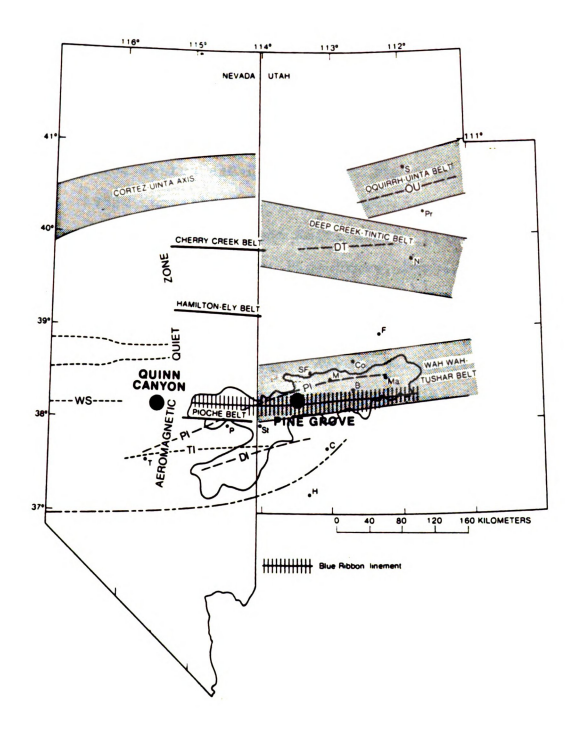


Figure 2. The Blue Ribbon Lineament and other mineral belts of eastern Nevada and western Utah (modified from Rowley et al, 1968).

Many workers recognize that fluorine-rich rhyolites are associated with, and may be indicators of, subsurface metallization, such as the economically important Climax-type stockwork molybdenum deposits in the western U.S. (Lamarre and Hodder, 1978; Westra and Keith, 1981; White et al., 1981; Burt et al., 1982; Christiansen et al., 1986; Keith et al., 1986).

Keith (1980 and 1982) and Keith et al. (1986) suggest that molybdenum mineralization at Pine Grove, Utah, is cogenetic with spatially associated extrusive high-silica rhyolite tuffs. The Pine Grove deposit is unique among major porhyry molybdenum deposits in having a direct correlation between eruptive and ore-bearing intrusive units. Because of its location and characteristics the Pine Grove mineralized system provides a possible "link" between the Climax-type stocks and ore bodies of the Colorado Mineral Belt and mineralization related to the emplacement of high level lithophile element-rich rhyolites in other areas of the western U.S., such as in the Quinn Canyon volcanic complex.

The Quinn Canyon volcanic complex exhibits many of the characteristics of economically significant mineralized systems, including some of the fundamental features of Climax-type districts. These features are: 1) the presence of high silica, apparently fluorine-rich peraluminous rhyolites, 2) anomalous concentrations of Mo, Pb, Zn, Sn, W, Au, and Ag dispersed in halos spatially and temporally associated with the rhyolite porphyry dikes and plugs, 3) fluorite and quartz veining associated with metal anomalies, 4) silicic, argillic,

potassic and propyllitic hydrothermal alteration, surrounding intrusive centers, 5) base-metal vein deposits, 6) precious metal bearing quartz veins, and 7) emplacement of high silica rhyolites coincident with the transition from compressional to extensional tectonics.

Although there are similarities between the Climax-type mineral districts and the Quinn Canyon Range, drill testing of one Mo-prospect in this area, has yielded generally negative results (Westjohn, personal communication).

The purpose of this investigation is to:

- Characterize the petrochemistry of the Quinn Canyon hypabyssal silicic rocks and evaluate possible genetic relationships among the rock types.
- 2) Evaluate the economic potential of the Quinn Canyon Range, by comparing the petrochemistry and source material of the Quinn Canyon rhyolites to that of the granitic and rhyolitic plutons that generated Climax-type porphyry molybdenum deposits and topaz rhyolites that are associated with volcanogenic Li, Be, U, and Sn mineralization.

Method

The following methods were used to address the problem:

1) The chemical composition of the Quinn Canyon igneous samples were determined by XRF (X-ray fluorescence) for major and selected trace elements and INAA (instrumental neurtron activation analysis) for rare earth elements (REE).

Petrochemical characterization of the suite of samples was accomplished by a series of major element variation diagrams, chondrite-normalized REE plots, and enrichment factor diagrams. Trace element composition and petrography were used to "group" the samples and to examine the relationships between the rocks of this suite.

2) Petrochemical comparisons of Climax-type granitioids with the Quinn Canyon rhyolite intrusives, were made possible by data generated at Michigan State University (Westjohn, 1985). A suite of samples from Urad-Henderson, Pine Grove, and Mt. Emmons, representing surface and subsurface samples, were analyzed for major and trace elements (including REE). The elements that appear to charaterized Climax-type plutons are Rb, Ba, Sr, Nb, Y, and Th (Westra and Keith, 1981). These elements, in combination with REE data, were used to make regional geochemical comparisons.

Pb isotope data from Zartman (1974), Stein (1985) and Stacey et al. (1968), and Nd-Sm isotope data published by Depaolo and Farmer (1984) provide a means of indirectly and directly comparing the source material of the igneous rocks and metallization associated with Quinn Canyon volcanic complex and Climax-type mineral districts.

PREVIOUS WORK

Sainsbury and Kleinhampl (1969) published the only written report on the geology of the Quinn Canyon Range with emphasis on the fluorite deposits. The authors describe the general geologic setting of the range including structure, plutonic and hypabyssal rocks, and sedimentary and extrusive volcanic rocks. Most importantly, Sainsbury and Kleinhampl produced a geologic map of the Quinn Canyon Range based on field work done between 1956-1965.

Kral (1951) describes in considerable detail the economic history of the range including locations of mines, types of ores, production, tonnage, and assays.

Lead isotope data from the Quinn Canyon Range is published in the appendices of Zartman's (1974) publication on the geologic significance of lead isotope provinces in the Western U.S.A. In addition, the Quinn Canyon Range is mentioned in the Rowly et al (1978) publication on the Blue Ribbon Lineament.

Economic evaluations were conducted by Amoco Minerals Co. in the early 1980's and will be discussed in a later section.

FIELD WORK

Field work was conducted over a 4 day period in September 1985. The focus of the field work was the sampling of hypabyssal and intrusive rocks, with emphasis on collecting fresh samples of rhyolite porphyry dike, plug, and flow rocks. The geological description of the study area, that follows, is based almost entirely on the work of Sainsbury and Kleinhampl (1969), with information added by D.B. Westjohn (1985). Sample locations are available in Appendix C.

GEOLOGY OF THE QUINN CANYON RANGE

The Quinn Canyon Range is located in southeastern Nevada, approximately 90 miles south and slightly west of Ely, Nevada (Figure 1). The Quinn Canyon Range is a distinctive unit of the Grant Range, separated from it by the Cherry Creek Canyon to the north (Kral, 1951; Sainsbury and Kleinhampl, 1969).

Tertiary extrusive volcanics and Paleozoic sedimentary sequences are the main rock-types that outcrop in the Quinn Canyon Range (Figure 1). Intruding these are a centrally located hypabyssal quartz-latite pluton (?) and a series of chemically variable dacitic-rhyolite porphyry dikes, plugs, and sills and andesite dikes (Sainsbury and Kleinhampl, 1969).

Sedimentary Rocks

The sedimentary strata is a typical eastern assemblage miogeosynclinal sequence (Sainsbury and Kleinhampl, 1969; Stewart and Poole, 1974; and Stewart, 1977). The exposed rocks are limestone, dolomite, shaly limestone, shale and quartzite of Early to Middle Paleozoic age, congolmerate and fresh water limestone of early to middle Tertiary age and tuffaceous sedimentary rocks (intercalated with volcanics) of middle to late Tertiary age (Sainsbury and Kleinhampl, 1969).

Igneous rocks

The extrusive units are primarily rhyolite and rhyolitic to quartz latitic welded tuffs of Oligocene and early Miocene age. Two of the units have tentatively been assigned to the Shingle Pass Tuff and the Needles Range Formation. The uppermost member of the Needles Range Formation has yielded a K-Ar date of 27.2 m.y., in the nearby Grant Range (Armstrong, 1970). The basal member, in other localities of Utah and Nevada has given consistent age values of 29.7 m.y. (Armstrong, 1970). Sainsbury and Kleinhampl suggest that the source area of the Needles Range Formation is to the east and the Shingle Pass Tuff to the northwest. A third undivided volcanic unit and a rhyolite tuff unit were mapped by Sainsbury and Kleinhampl (1969). Andesitic and basaltic breccias and flows are found at the base of the volcanic pile. The volcanic stratigraphy is poorly understood.

The dacitic to rhyolitic dikes range from several inches to greater than 300 feet in width, and are emplaced along east northeast trending fractures. They cut the Paleozoic sedimentary package and most of the Tertiary volcanic sequence (Sainsbury and Kleinhampl, 1969). A K-Ar date of 23 m.y. has been obtained for alteration associated with one rhyolite intrusive center (Westjohn, personal communication, 1985). Sainsbury and Kleinhampl assume that the quartz latite hypabyssal "stock" is genetically related to the various rhyolitic dikes and plugs. This assumption will be examined in later chapters. A granite stock, located in the northwest

portion of the study area, is believed to be older than both the rhyolite porphyry dikes and the quartz latite stock (Sainsbury and Kleinhampl, 1969; Westjohn, personal communication, 1985).

Structure

The Quinn Canyon Range is composed of a series of blocks that are bounded by Basin and Range faults. Paleozoic rocks outcrop in blocks to the north and east in the study area. Both high angle and thrust faults occur, with the thrust faults appearing to pre-date volcanic activity.

High angle faults appear to be more dense and complex in the Paleozoic section, then those observed in the Tertiary sequence. Sainsbury and Kleinhampl (1969) suggest that faults in the Tertiary volcanic units are difficult to identify, implying that high angle faulting in the Tertiary may be more prevalent than their maps suggest.

The contact between the Paleozoic and Tertiary rocks is enginatic. Sainsbury and Kleinhampl report that in some cases the sharp contact does not appear to be fault related, but is depositional in nature. They cite the area north of Adaven as an example of where Tertiary volcanics appear to lie on the prevolcanic surface. There is evidence of fault contacts near the High grade, Spar, and Mammoth properties. Faults in this area seem to be a major structural feature of the range (Sainsbury and Kleinhampl, 1969).

Economic Geology

The Quinn Canyon Range has been the subject of sporadic mining activity and exploration interest since 1971 (Kral, 1951). Although there has been production from numerous small mines, the return from these workings has been relatively insignificant with no major deposit of economic significance known to date. Kral (1951) estimates that the total production amount at that time was less than \$100,000.

Three main types of deposits have been recognized by previous workers. They are: 1) fluorite replacements and veins; 2) base metal deposits; and 3) gold-bearing quartz veins (Kral, 1951; Sainsbury and Kleinhampl, 1969).

Native gold occurs in quartz veins, frequently with arsenopyrite. The majority of the gold deposits are located in limestone near Willow creek, and appear to be associated with a quartz monzonite stock (Kral, 1951; Sainsbury and Kleinhampl, 1969). Kral also describes a gold vein adjacent to an andesite dike in this area.

Although little description is available for the base metal deposits, Kral states that the minerals are typically arsenopyrite, sphalerite, pyrite, galena, and occasionally tetrahedrite, which occur in veins and at least in one instance are associated with a large rhyolite dike.

The fluorite deposits have been studied in considerable detail by Sainsbury and Kleinhampl (1969). The authors describe eight fluorite deposits and mention that numerous prospects are scattered throughout the range. The deposits

are grouped into two types; those that occur as veins and tabular replacement bodies in carbonates, and a less economically important and less diverse group occuring as fissure veins and tabular bodies in volcanic rocks. The fluorite is spatially associated with rhyolite dikes as well as deposited along faults. In the volcanic rocks, fluorite veins are found within altered zones. Sainsbury and Kleinhampl state that the alteration zones in the Cottonwood area are up to 4,000 feet long and 500 feet wide and locally parallel fault zones. The alteration zones as a group define a northwest trending band that may be aligned along a major Pre-Tertiary fracture zone (Sainsbury and Kleinhampl, 1969).

The Quinn Canyon Range, was the target of exploration activity in the late 1970's and early 1980's. Amoco Minerals Co. initiated a reconnaissance exploration program in 1980, with a more detailed study in 1981-1982, which included geologic mapping, geochemical sampling and geophysical surveying (Westjohn, personal communication, 1985).

Amoco has provided geochemical data and maps for this study, which will be integrated into a brief summary of the key geochemical anomalies in the range. Rock chip and stream sediment samples were analyzed, by Amoco for at least some, and in many instances almost all of the following elements; Au, Ag, As, Hg, Sb, Sn, Pb, W, Zn, Ba, Mo, F, and Mn.

Eight different hydrothermally altered centers that are spatially associated with rhyolite intrusives have been recognized by Amoco Minerals in the Quinn Canyon Range (Westjohn, personnel communication, 1985). Surrounding these

intrusive centers are specific and somewhat exclusive metallogenic halos. Four of these areas have been studied in detail by Amoco and display distincly different enrichment trends. The anomalous elemental suites are: 1) Mo and F, 2) Mo, Sn, Pb, Zn, W, Ag, and F, 3) Mo, Pb, Zn, Ag, and F, 4) Mo, Ag, Au, and F (Westjohn, personal communication, 1985). There is a change in the elemental distribution pattern from one area to another in the Quinn Canyon Range. This change is subtle, but in the case of the second and fourth elemental halos, the presence of Sn and Au is distinctive. These differences may be due to variations in source igneous rock chemistry, and/or type of country rock (Paleozoic sedimentary vs. Tertiary volcanic).

The intrusive center marked by presence of anomalous Sn (up to >1000 ppm) is located in the extreme eastern portion of the range and is composed of several rhyolite porphyry dikes and a large sill (area 1 of Figure 1). In addition to the elements mentioned previously, somewhat anomalous W (mostly <10 ppm, one 100 ppm value), and Mn (to > 10,000 ppm at the Roadside Mine) are characteristic of this suite. Mo ranges from 7-53 ppm, Pb values consistently over 4000 ppm (particularly in the southern portion of this area), F> 10,000 ppm and Ag reaching concentrations greater than 20 ppm.

The region with consistently high Au and associated element (As, Ag, and Hg) values is in Water Canyon, in the western portion of the study area (area 2 of Figure 1). In this location Mo occurs in isolated concentrations greater than 400 ppm, predominately in quartz veins. Au values of

over 1 ppm and Ag values as high as 50 ppm are recorded, although the majority of samples have much lower concentrations. The highest concentrations of the previously mentioned elements were for the most part from rock chip samples of country rock, with quartz veins, although intrusive rock samples were moderately to highly enriched in some of the elements of economic interest. Field evidence suggests that the metals were carried in fluids exsolved from the crystallizing silicic porphyry intrusives and deposited in the country rock.

A total of seven rotary drill holes were drilled in Water Canyon by Amoco Minerals Co., during 1982. Six of these exploration holes were relatively shallow (200'-500'), and bottomed in Tertiary rhyolite tuff. The drilling consistently indicated stockwork quartz veining, weak-moderate silicification and pyritization, localized zones of weak-moderate argillic alteration and trace MoS2.

The seventh drill hole was completed to a depth of 1024 ft and cored from 440 ft to the bottom. Silicified and locally argillized Tertiary rhyolite tuff, with associated quartz-latite lithic fragments was encountered in core from 474 ft to 860 ft. In this interval, stockwork quartz-pyrite-fluorite veins were common with pyrite exceeding 1% in most core intervals, and locally exceeding 17%. MoS2 (Jordisite) was identified in quartz veins. Propyllitic alteration, characterized by chlorite and quarz-pyrite-calcite veins was observed from a depth of 790 ft-864 ft argillically altered quartz-latite occured at a depth of 864 ft-880 ft,

with intense quartz-calcite-pyrite-fluorite veins from 874 ft-880 ft. Chlorite altered rhyolite intrusive breccia extended from a depth of 880 ft-914 ft. A lithic-poor fractured rhyolite was encountered from 914 ft-934 ft, followed by a rhyolite porphyry intrusive (?), featuring resorbed bipyrammidal quartz phenocrysts in a glassy matrix.

Geochemical analysis of core samples, revealed anomalously high Mo values at 516 ft (112 ppm) and 791 ft (885 ppm).

PETROGRAPHY

The following petrographic summary will focus on the silicic hypabyssal, extrusive dome and flow rocks collected in the Quinn Canyon Range. Three groups can be crudely delineated, based on petrography. For ease of description these groups are named:

- 1) rhyolites
- 2) less evolved or low silica rhyolites
- 3) rhyodacites

Within the rhyolite group two smaller populations can be delineated according to major and particularly trace mineral phases. See Table 1 for sample numbers and brief descriptions of each group.

Mineralogy and texture

The rhyolites range from distinctly porphyritic to aphyric and predominately have euhedral to subhedral phenocrysts of quartz, potassium feldspar (orthoclase) and subordinate amounts of plagioclase (albite-oligoclase). These samples either have a matrix composed of entirely recrystalized spherulitic alkali feldspar and quartz intergrowths, or a combination of this texture occurring as "patchs" within a

Petrography of the Quinn Canyon silicic rocks. Table 1.

Group	Mineralogy	Samples
1. Rhyolites	Major phases: potassium feldspar, plagioclase (albite-oligoclase), quartz Trace phase: zircon, sphene, apatite, opaques, biotite, fluorite (Qc-8)	Oc-16, Oc-19a, Oc-15, Oc-8, Oc9-5, Oc9-4, Oc-14, Oc-6, Oc -1a, Oc-12
1a. Muscovite-bearing rhyolites	Major phases: potassium feldspar, plagioclase, quartz Trace phases: muscovite	Qc9-9, 2016, 2012, 2015, 2010, 2011, 2008, Qc-5, 2007, 2022
1b. Highly evolved rhyolites	Major phases: quartz, potassium feldspar, albite Trace phases: biotite (Qc-19), fluorite (Qc-19c)	Qc-19c, Qc-19, Qc-20, Qc9-3, Qc-13
2. Low silica rhyolites	Major phases: potassium feldspar, plagioclase (oligoclase-andesine), quartz biotite (highly altered), amphibole (highly altered) Trace phases: zircon, apatite, opaques	Qc-11a, Qc-11b, Qc-9e, Qc-9b, Qc-9c, Qc-10, Qc15n, Qcjw4b
3. Rhyodacites	Major phases: plagioclase (andesine), potassium feldspar, biotite (altered), amphibole (highly altered) Trace phases: apatite, zircon	Qc-3a, Qc9-1, Qc9-2

	Silification	2007, Qc-5, 1109, 1107, 1102b, 1001
Alteration	Argilization	Ocjw2a, Ocjw2b, Ocjw2c
	Other types of alteration seen to some degree in most samples—chloritization, sericitization and replacement by and addition of calcite.	

cryptocrystalline or microcrystalline matrix. These spherulites often occur as halos radiating out from and surrounding phenocrysts. Micrographic intergrowths of alkali feldspar and quartz are also pervasive in the matrix of many of the samples. Resorbed quartz grains are common. Plagioclase phenocrysts exhibit albite twinning, are generally unzoned, and in some instances have alkali feldspar overgrowths. Accessory minerals include: zircon, sphene, apatite, opaques, and biotite.

A distinct series of rhyolite samples contain primary(?) euhedral to subhedral muscovite in significant concentrations in the groundmass and lack spene and zircon.

Another subgroup appear to be the most "evolved" of the rhyolite population and are characterized by a large portion of euhedral-subhedral quartz phenocrysts relative to potassium feldspar and albite. Some of these phenocrysts exhibit a graphic intergrowth of quartz and alkali feldspar. Embayed quartz phenocrysts are prevalent. This group of rhyolites has a microcystalline matrix of albite, quartz, and potassium feldspar with samples Qc-19c and Qc9-3 having the spherulitic groundmass as seen in many of the other rhyolites. Qc-19 is the only rock of the group to have significant amounts of sanidine and trace amounts of relatively unaltered biotite. Biotite in Qc-19, and fluorite in Qc-19c and Qc9-3, appear as accessory mineral phases. Muscovite, with the exception of a small amount in sample Qc-20, zircon, and sphene are absent.

The less evolved rhyolite dike samples were all collected in the same general area. They differ from the rest of the silicic rocks by having a large amount of plagioclase phenocrysts (oligocene-andesine), and potassium feldspar phenocrysts, few, if any quartz phenocrysts and a significant amount of altered biotite and amphibole(?). Accessory minerals include zircon, apatite and opaques.

The three rhyodacite samples taken from the quartz latite plug exhibit marked extrusive, and in one instance flow-like texture. Many of the phenocrysts are broken and angular, and in sample Qc9-1 are crudely aligned. The phenocrysts phases present include; large, embayed, and in some cases broken quartz grains, highly altered plagioclase (andesine), potassium feldspar, biotite and amphibole.

Alteration

The degree and type of hydrothermal alteration varies from sample to sample, but all of the silicic rocks collected at Quinn Canyon are altered to some degree. The principal types of hydrothermal alteration are silicification, sericitization, the addition of and replacement of mineral phases by calcite, and to a lessor degree, argillization and chloritization (Table 1).

Typical alterations are: plagioclase to sericite and calcite, alkali feldspar to clays and chlorite, biotite and amphibole to chlorite (some penninite), amphibole to epidote, the silicification of major mineral phases, as phenocrysts and

in the groundmass (primarily plagioclase and alkali feldspar) and quartz veining. Generally, the highly evolved rhyolites (Qc-19, Qc-20, etc.) are primarily silicified, while the other rhyolites and rhyodacites, in addition to being silicified, have calcite, sericite and chlorite as alteration products.

With several exceptions, this rock suite shows a weak to moderate amount of alteration, and as such, most of the trace elements and many of the major elements should reflect approximate magnatic concentrations.

PETROCHEMISTRY

Major elements

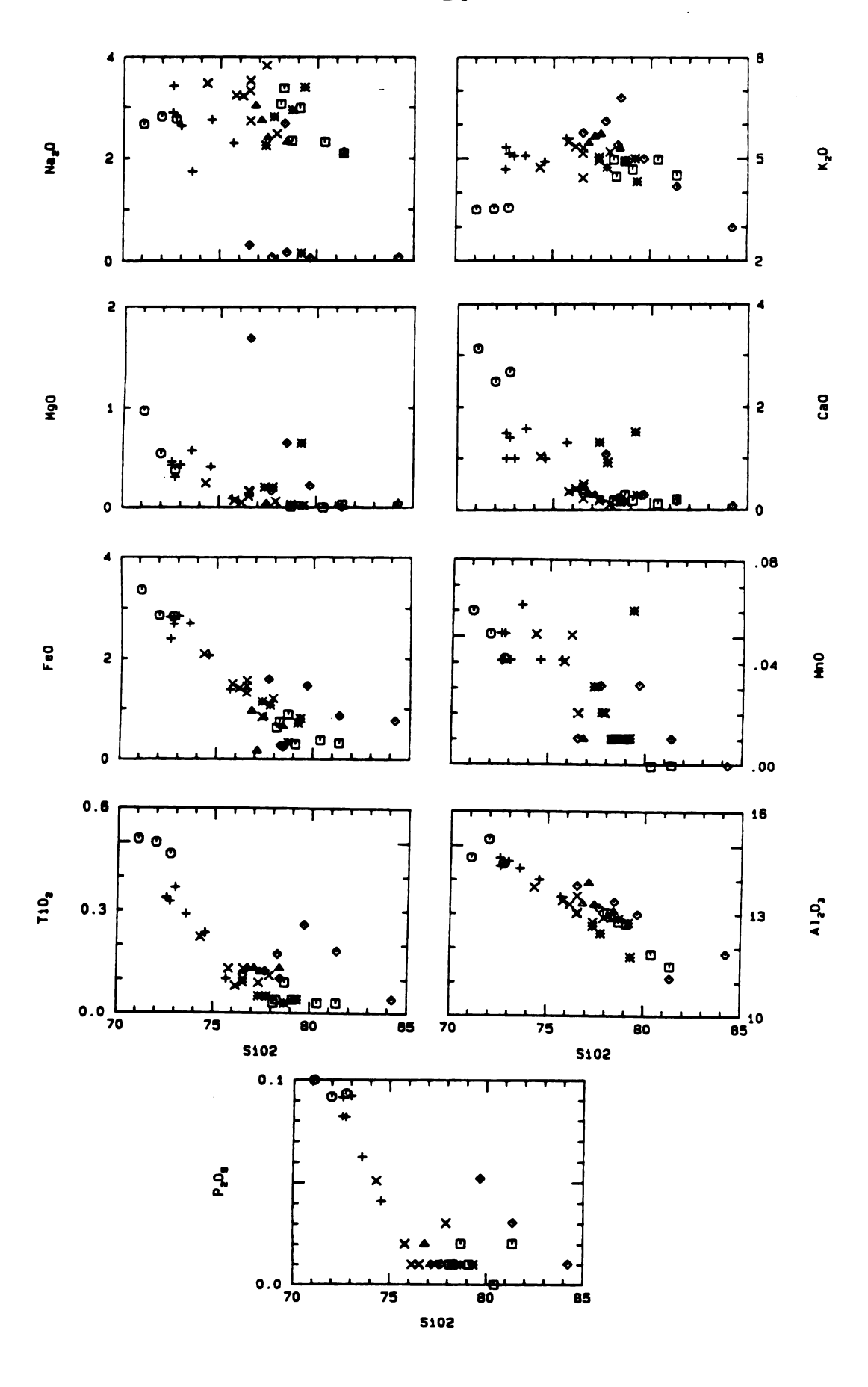
The chemical data for all rocks are presented in Appendix A, by methods described in Appendix B. The silicic rocks collected from the Quinn Canyon Range are peraluminous rhyolites and rhyodacites. The "freshest" most evolved rhyolites have K20 values which range from 4.32%-5%, Na20 values from 2.25%-3.4% and are depleted in CaO (generally less than .2%), MgO (<.03%, frequently not detected), P205 (.01%) and TiO2 (<.04%). K20/Na2O ratios range from 1.2-2.4 for relatively unaltered rocks of the entire suite. Silica values are variable (72% to >80%) depending on the degree of alteration and differentiation. Major element variation diagrams are shown in Figure 3. Group divisions are based primarily on trace element chemistry as outlined in a following section.

Alteration

The majority of the scatter and extreme deviation of the major element oxides can be easily attributed to alteration.

The affects of alteration on major element chemistry are twofold: first, the addition of major cations through alteration and secondly the addition of non-measured ions such

Figure 3. Major element variation diagrams for the Quinn Canyon silicic rocks. Highly altered samples are denoted by a \diamondsuit . See figure 5 for group symbols.



as C (in CaCO₃), F (in CaF₂) and structurally bound H₂O. The addition of significant amounts of H₂O, CaCO₃ and/or CaF₂ is recognized by either anomalously high CaO values and/or anomalously low measured major element oxide totals.

Silicification and argillization are common alteration types that produce in the first instance an increase in SiO2, and in the second case, an increase in K2O and a decrease in Na2O. The addition of calcite and the alteration of feldspars to sericite and chlorite also cause some scatter in the plots of CaO, K2O, MgO and Na2O.

Samples that consistently deviate from the "trend" in major and selected trace element variation diagrams, such as Zr, Eu and Sr vs SiO2, and/or exhibit extensive alteration in thin section, were not included in group comparisons (Figures 3 and 4). The small grouping of samples with the lowest silica values are not highly altered, but rather are significantly less "evolved".

Samples that show minimal amounts of alteration, such as the small amount of silicification seen in some of the more evolved rhyolites were used in trace element comparisons.

Most workers believe that under many alteration conditions (including hydrothermal alteration), the elements Nb, Y, Sc, Hf, Zr, Ti and REE, particularly heavy rare earth elements (HREE) are relatively immobile (Winchester and Floyd, 1977; Floyd and Winchester, 1978; Campbell et al., 1984; Palacious et al., 1986; and Maclean and Kranidiotis, 1987). Other workers maintain that under extreme hydrothermal alteration,

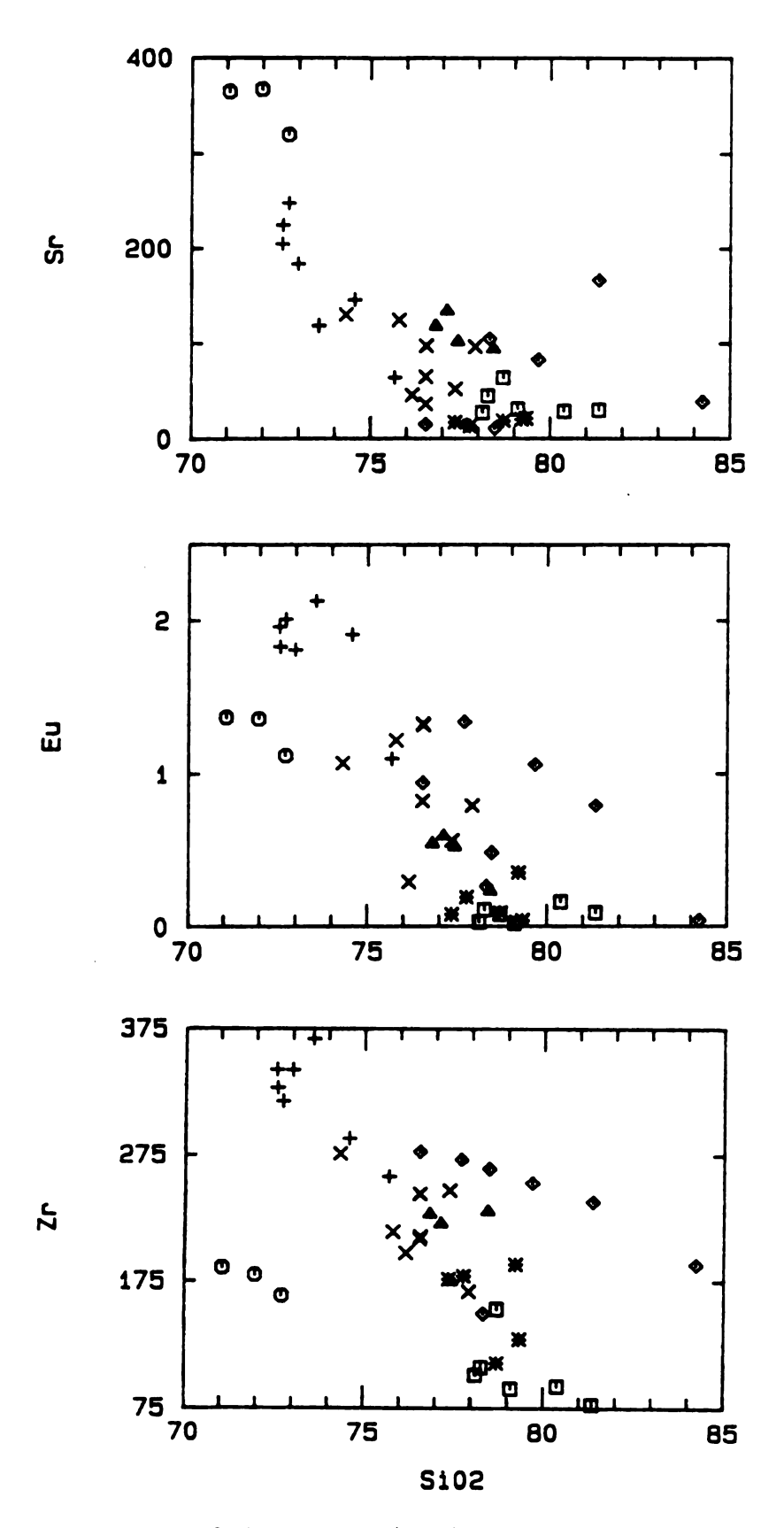


Figure 4. Plots of Sr, Zr, and Eu vs SiO2 for the Quinn Canyon rocks. Highly altered samples are denoted by a . See figure 5 for group symbols.

Y, Sc, Nb, and REE can be significantly mobile (Alderton et al., 1980; Finlow-Bates and Stumpfl, 1981). They suggest that only Zr and Ti are immobile and can be used to identify the degree of magmatic differentiation in a hydrothermally altered rock. These authors have described and studied the results of extreme alteration. Except for a small group of highly altered samples, the general weak to moderate alteration exhibited by the Quinn Canyon rocks should have little influence on trace element chemistry, particularly Y, Nb, Zr, Hf, Ti and HREE.

Trace elements

The Quinn Canyon rhyolitic rocks can be "grouped" according to trace element chemistry, particularly REE chemistry. The arthimetic mean of selected trace element concentrations for each group are presented in Table 2. The differences in trace element composition between groups can be attributed to variability in source material and/or degree of igneous processes, such as partial melting and crystal fractionation. With the exception of one group, samples within each group are assumed to be genetically similar. Different degrees of alteration, partial melting and crystal fractionation are probably the cause of variation that exists in some groups.

Six groups can be roughly defined and named for ease of description and comparison. The "justification" for these groupings was evaluated by R-Mode factor analysis. Initially,

Arthimetic mean of selected trace elements for the Quinn Canyon Table 2. groups.

QUINN CANYON GROUPS

	Rhyodacites (3)	Low Silica Rhyolites (6)	Rhyolites (6)	Muscovite-Bearing Rhyolites (Group 2) (4)	Muscovite-Bearing Rhyolites (Group 1) (6)	Incompatible Element-Rich Rhyolites (5)
æ	919	1150	614	928	130	169
8	147	169	196	231	261	370
£	14	25	32	23	23	72
<u>.</u>	31	69	20	21	9	18
Sr	351	188	08	112	38	18
Ä	1.3	1.9	o:	۸i	80.	.15
Sm	5.8	10	9.1	3.6	2.2	11
Z	178	331	218	213	104	157
TiO2	.05	.32	.12	.13	Ş.	3 .
>	19	41	20	30	42	117
ç	1.8	1.2	3.8	2.4	3.2	6.4

runs using all chemical variables, grouped the samples in similar clusters. Later runs, in which chemical variables which had similar loadings were deleted, left essentially the same clusters. These clusters were grouped according to Rb, Sm, La, Sr, and SiO2 as the dominant variables. The six groups are:

- 1) rhyodacites
- 2) low-silica rhyolites
- 3) rhyolites
- 4) muscovite-bearing rhyolite group 1
- 5) muscovite-bearing rhyolite group 2
- 6) the most "evolved" or incompatible element-rich rhyolites.

Sample numbers and trace element compositions are presented in Appendix A. This grouping of samples is evident in many trace element plots, and is well illustrated in plots of La vs Y, and Zr vs Y (Figure 5). The identification of samples as rhyodacites and rhyolites is loosely based on a classification scheme according to the position of samples on a Zr/Ti vs Nb/Y plot (Winchester and Floyd, 1977).

The composition of several chemically variable, generally silicified rhyolites (1102b, 1001, 1107, and 1109) taken from the western portion of the Quinn Canyon volcanic complex (Water Canyon) are presented in Appendix A, but will not be included in the following comparisons.

An enrichment factor diagram of the mean of the groups, normalized to U.S.G.S. standard RGM-1, was used for displaying element distribution patterns and for group comparisons

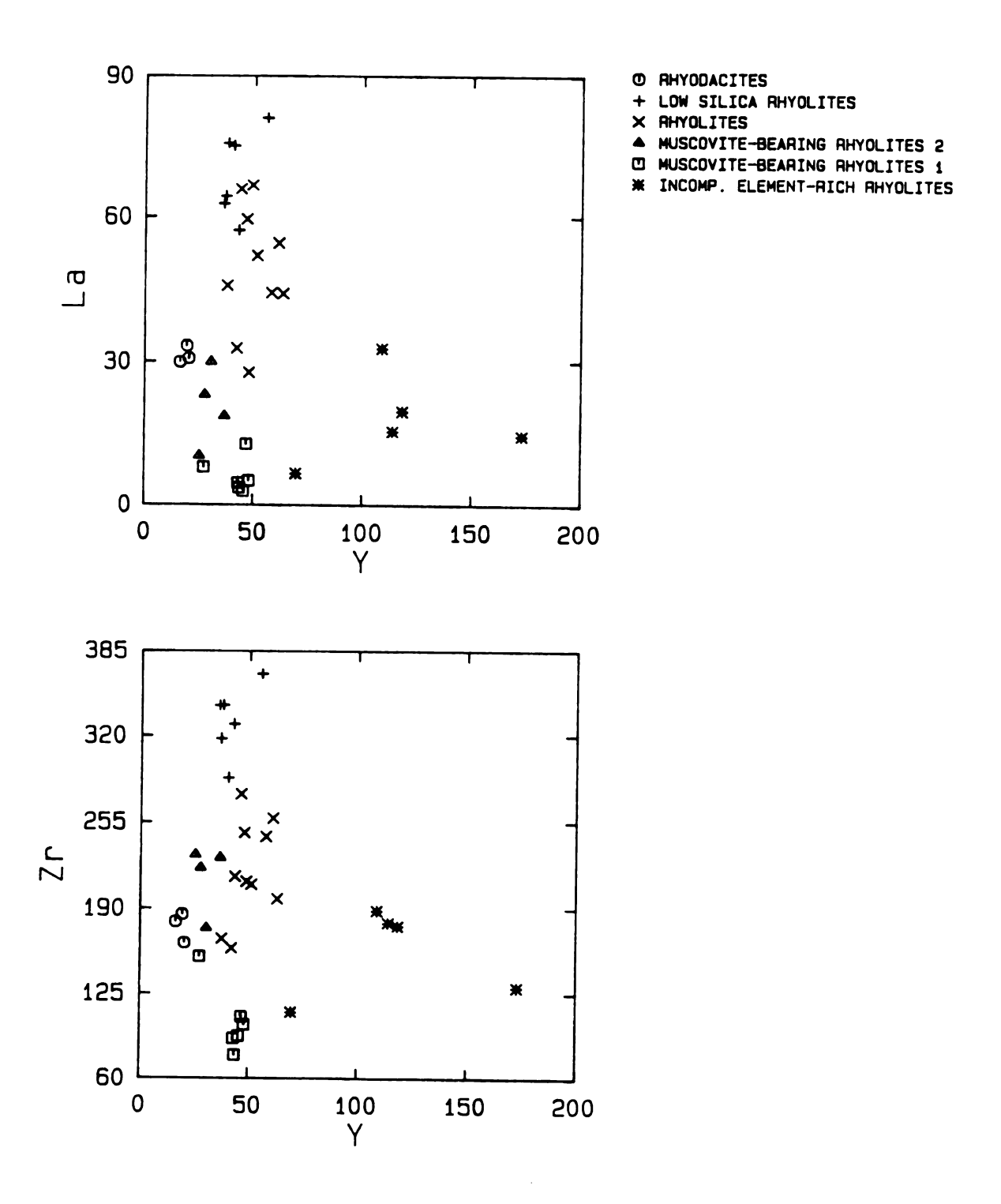


Figure 5. Plots of La and Zr vs Y the Quinn Canyon sample groups.

(Figure 6). RGM-1 is a rhyolite obsidian from Medicine Lake Volcano, California and was used by Christiansen et al (1986) for characterizing topaz rhyolite trace element chemistry. The elements of this plot are arranged with increasing field strength to the right, after Pierce et al. (1984) and Christiansen et al. (1986).

The three rhyodacite samples comprising the least evolved group were collected from the large centrally located "quartz latite" dome in the Quinn Canyon Range. Compared to the other silicic rocks of this suite, these samples are depleted in Rb, Y, Nb, and Th and enriched in Eu, and Sr (Figure 6). The REE distribution pattern roughly parallels that of the group of low silica rhyolite dikes, having a small negative europium anomaly, La/YbN of 9-11, but with overall lower chondrite-normalized abundances (Figure 7).

The series of low silica rhyolite dike samples display a consistent trace element chemistry, having subequal proportions of Rb and Sr, being depleted in Nb, Y, Th and enriched in Eu, Ba, REE elements, particularly light rare earth elements (LREE), Zr and Hf, relative to the most evolved rhyolites of this suite (Figure 6). This group has a straight line REE pattern, with a small negative Eu anomaly. La/Ybw ratio averages about 13 (Figure 7).

The rhyolite group shows the most chemical variation. It is characterized by a La/Ybw ratio of 4-12, Sm/Yb ratio of 2-3, and an enrichment trend which, in general, lies between the low silica rhyolites and the highly evolved rhyolites (Figures 6 and 8).

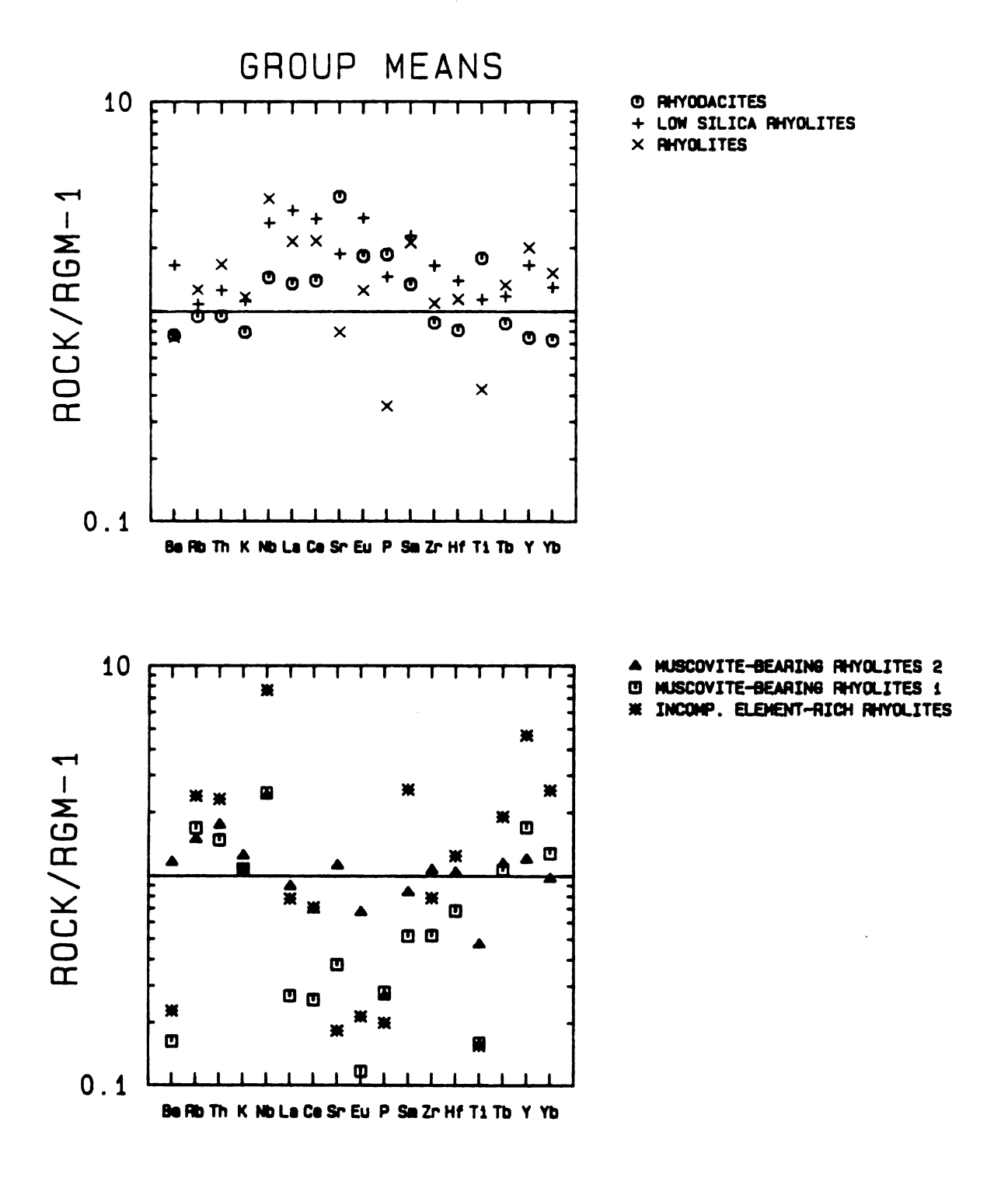
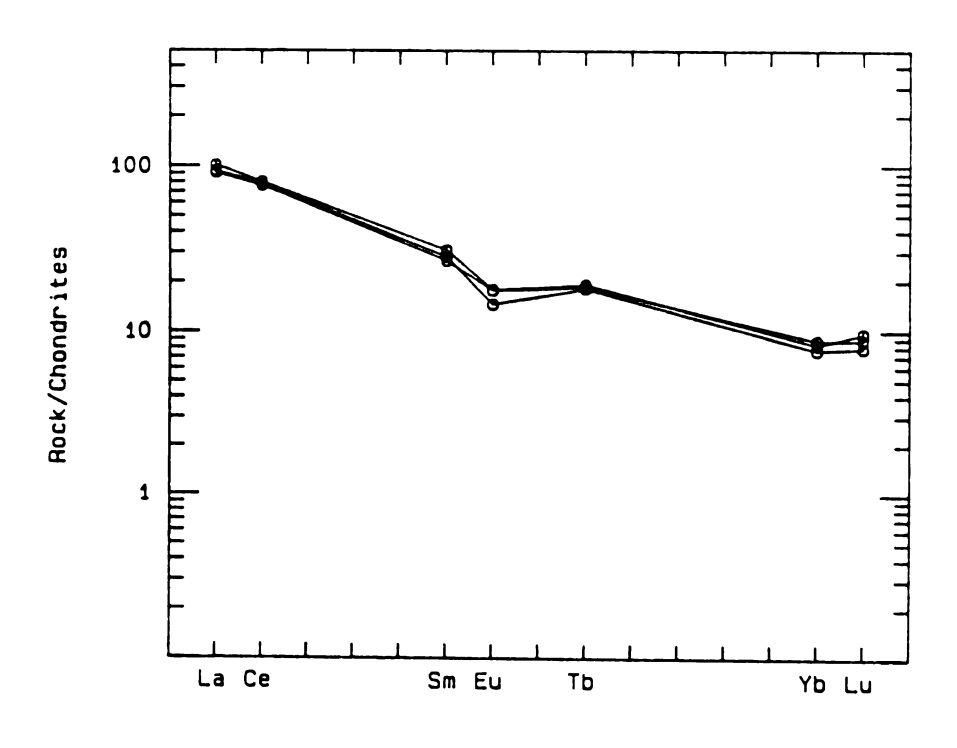


Figure 6. Arthimetic mean of selected trace elements of the Quinn Canyon sample groups, normalized to U.S.G.S. standard RGM-1 (rhyolite).

RHYODACITES



LOW SILICA RHYOLITES

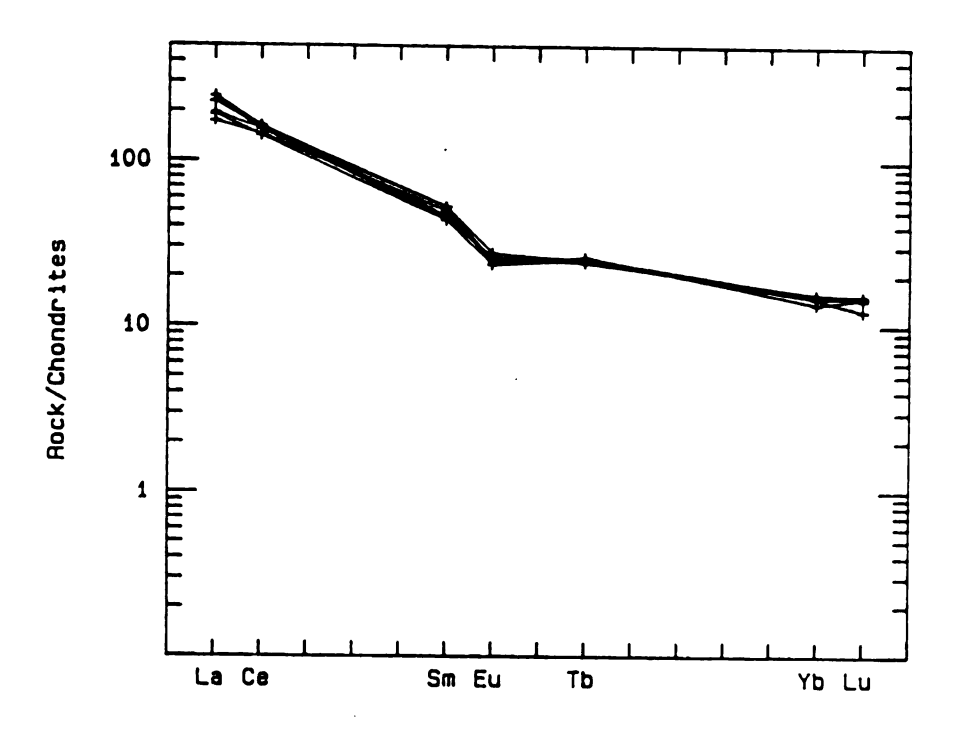
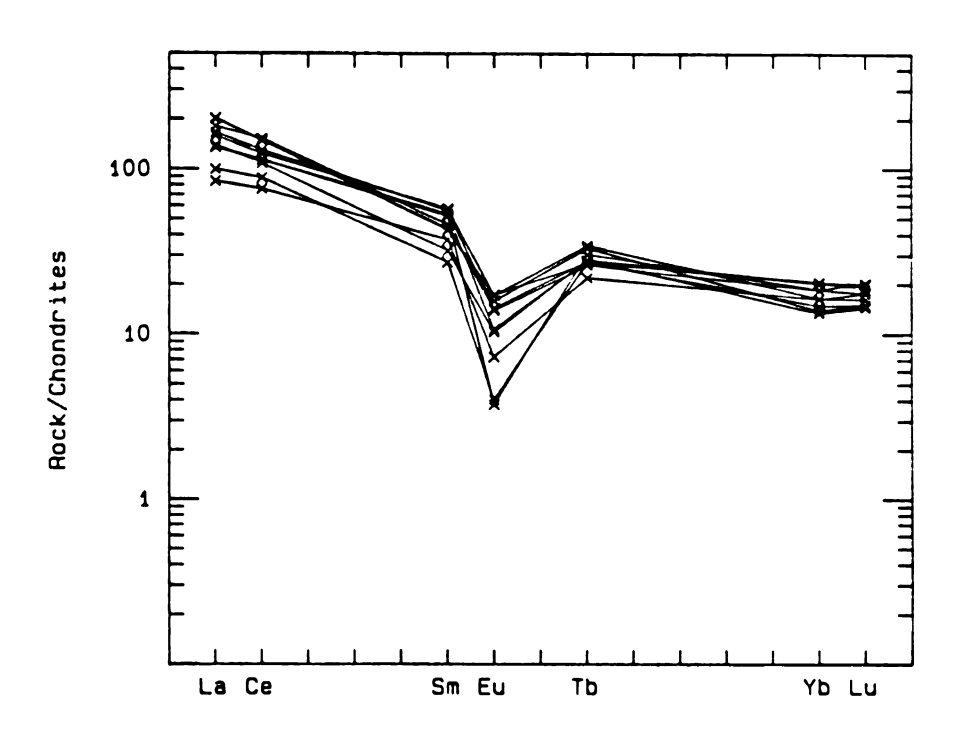


Figure 7. Chondrite-normalized REE patterns for the rhyodacites and low silica rhyolites.

RHYOLITES



INCOMPATIBLE ELEMENT-RICH RHYOLITES

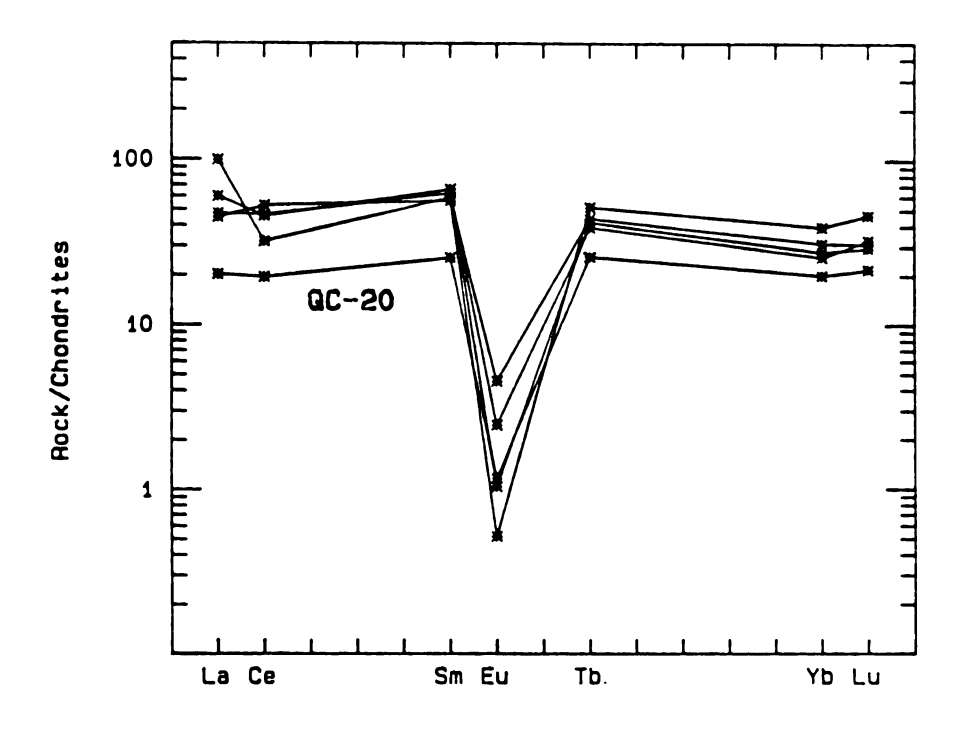
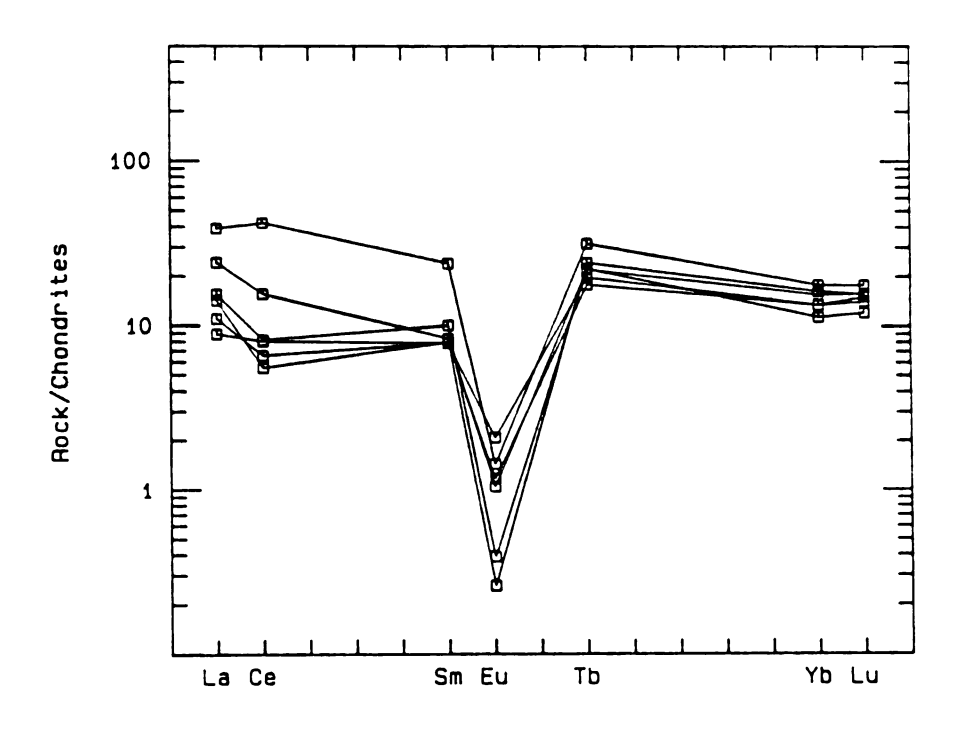


Figure 8. Chondrite-normalized REE patterns for the rhyolites and incompatible element-rich rhyolites.

MUSCOVITE-BEARING RHYOLITES GROUP 1



MUSCOVITE-BEARING RHYOLITES GROUP 2

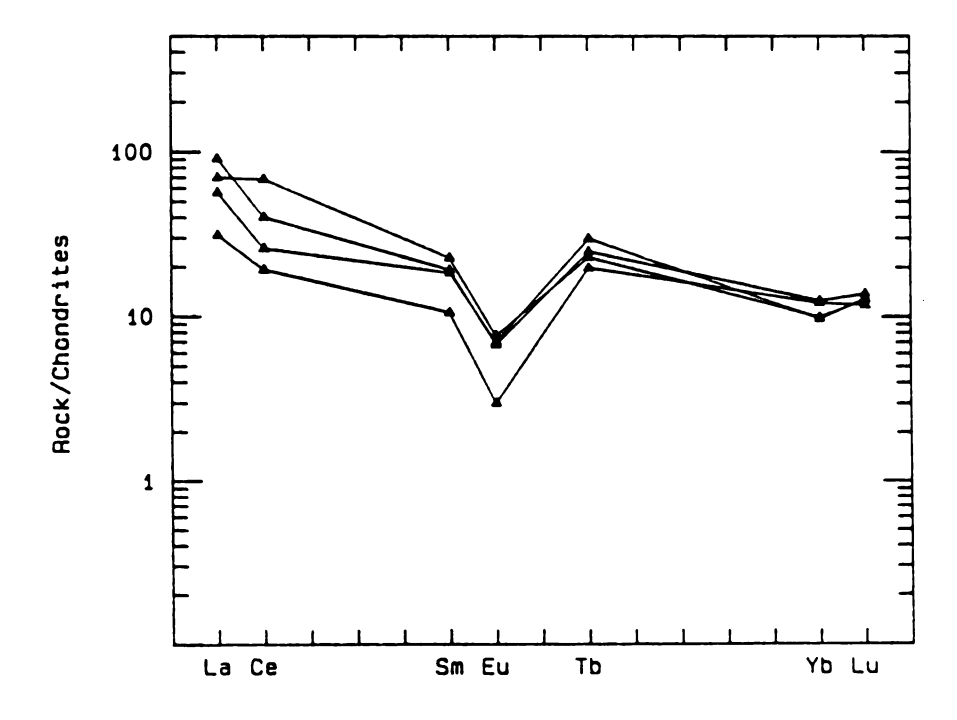


Figure 9. Chondrite-normalized REE patterns for the muscovite bearing rhyolites group 1 and 2.

The first group of "muscovite-bearing" rhyolites, marked by the presence of muscovite in most samples, are distinctly depleted in Zr, Hf, Eu, Ba and Ti, and slightly enriched in With the exception of the rhyodacite group, these rhyolites show no enrichment in the incompatible elements Nb and Th relative to other silicic rocks of this suite. This group also displays anomalously large LREE and middle rare earth elements (MREE) depletions, with La/Ybn ratios of .5-2 and Sm/Ybw ratios of .5-1.5 (Figures 6 and 9). The low Ti, Eu, and Ba concentrations, suggest a significantly differentiated or "evolved" rhyolite, much like the group of incompatible element-rich rhyolites described below. The peculiar extreme depletion in LREE and MREE could be a result of extreme differentiation of light and middle REE-rich mineral phases, a reflection of the source material, and/or possibly a result of alteration. Possibly related to this group are several "less evolved" samples (muscovite-bearing rhyolite group 2), some with muscovite, which have higher REE abundances, yet display a similar tendency for MREE depletion. These rhyolites are more enriched in Ti and Zr (Figures 6 and 9).

The most evolved or incompatible element-rich rhyolites of the Quinn Canyon range are distinctive in having a large negative Eu anomaly, a "flat" REE distribution pattern (La/YbN ratio 1-3) and are extremely enriched HREE, Nb, Y, Rb, and Th and depleted in Sr, Ba, Hf, Zr, and LREE (Figures 6 and 8). Overall REE abundance is greater than the previously described muscovite-bearing rhyolite group 1. This type of

trace element signature is typical of other highly evolved, incompatible element-rich rhyolites of the Western U.S. (Burt et al., 1982; Christiansen et al, 1986). The LREE depletion is probably due to the fractionation of LREE-rich trace mineral phases such as allanite, monazite, and chevkinite. A contributing factor to the low La/Yb ratio could be that HREE complex more readily with fluorine, and may be preferentially enriched in the roof of a fluorine-rich magma chamber, during convection-driven thermogravitational diffusion as suggested by Hildreth (1979). The low Hf and Zr values are probably due to their compatibility with fractionating zircon. Likewise, the Ba depletion may be due to the fractionation of potassium feldspar.

Mo, Pb, and Sn were analyzed for rhyolites of this group and display a general negative correlation of Pb, with Mo and Sn (Figure 10).

Sample Qc-20 is unique in having trace element characteristics of both the previously mentioned group of rhyolites and the muscovite-bearing rhyolite group 1.

Specifically, it is enriched in Rb, somewhat enriched in Y and Th and shows little Nb enrichment. This sample has a low La/Ybw ratio (1) and an overall low REE abundance (Figures 6 and 8).

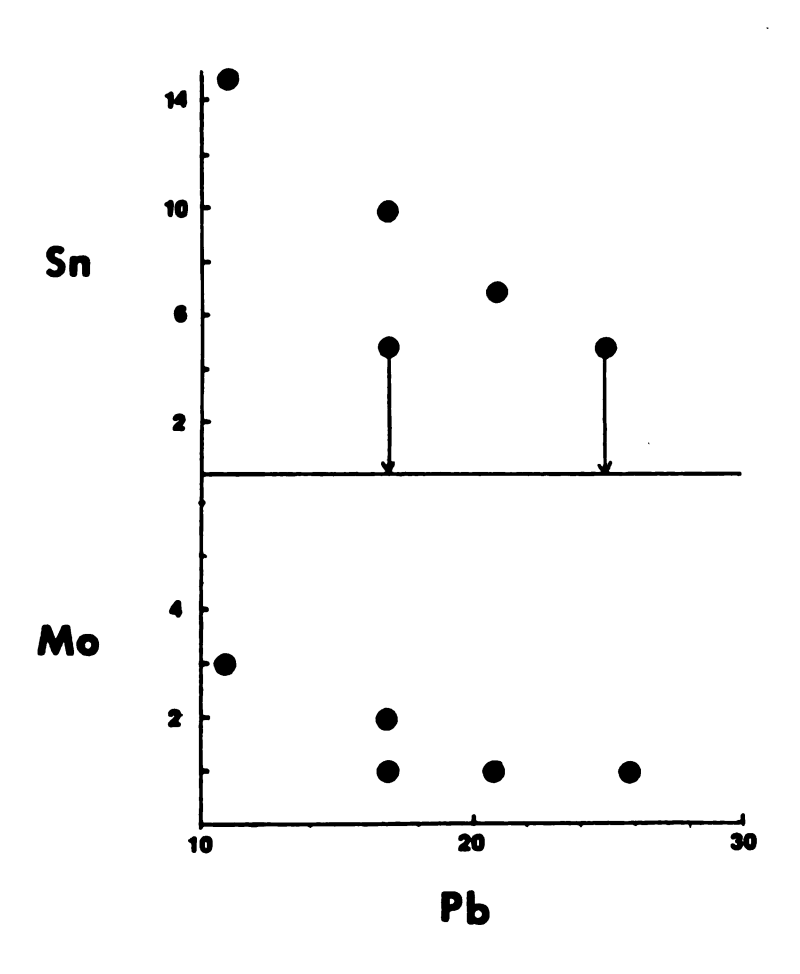


Figure 10. Plots of Mo and Sn vs Pb for the incompatible element-rich rhyolites. Analyses done by Bondar & Clegg Ltd.

Fluorite

The trace element composition of a fluorite sample taken from an open pit just west of the Hi Grade Prospect, is included in Appendix A.

REGIONAL GEOLOGY

Lineaments

Several east-west trending mineralized belts and structural linaments have been recognized in Utah and Nevada, based on aeromagnetic data; fluorine, tungsten, berylium, uranium and base metal mineralization; hydrothermal alteration, and the presence of Tertiary eruptive and hypabyssal centers (Rowly et al., 1978; Stewart et al., 1977; and Shawe and Stewart, 1976). The best defined belts are the Deep Creek-Tintic belt of Central Utah, the Qquirrh-Unita belt of north central Utah and the overlapping Wah-Wah-Tushar belt, Pioche belt and Blue Ribbon Lineament of south central Utah and eastern Nevada (Rowley et al., 1978). The Blue Ribbon Lineament has been defined by Rowly et al. (1978) as a distinct structural zone within the Pioche belt as defined by Shawe and Stewart (1976) (Figure 2).

Rowly et al. (1978) and Stewart et al. (1977) concur that these lineaments may be due to an east-west trending structural warp or break in the subducting slab. Rowly et al. (1978) suggest that the fractures associated with the Blue Ribbon Lineament (BRL) were important conduits for mineralizing solutions or, more accurately, acted as zones of weakness for emplacement of rhyolitic-granitic rocks which were the source for mineralization. In any event, as the

authors emphasize, the BRL has important exploration significance.

The Quinn Canyon Volcanic center is located along trend at the western end of the BRL and Pioche belts in the Quiet Zone (Rowly et al., 1978). The Quiet Zone (QZ) is a north-south oriented area from about 115 to 116 W., where the aeromagnetic signature, characteristic of the BRL and other mineral belts, is absent (Figure 2). This zone is puzzling because relatively large volumes of intermediate calc-alkaline igneous rocks outcrop here and these types of igneous rocks are associated with high intensity positive magnetic anomalies in other areas within the BRL.

Stewart (1976) and others suggest that perhaps few large intrusive bodies exist in the Quiet Zone, even though large volumes of extrusives are present (in the Quinn Canyon Range this may be supported by Sainsbury and Kleinhampl's conclusion that a large portion of the extrusive sequence is sourced from the east and northwest). Also, they suggest that the QZ is located in and parallel to a thick portion of the miogeosynclinal sequence as noted by Stewart and Poole (1974). Rowly et al. (1978) believe that the lineament passes through the QZ based on the nature of the surface geology and the presence of fluorite and base metal deposits in the Quinn Canyon Range. The Warm Springs lineament is just west of Quinn Canyon and on trend with the BRL, lending support to the theory that the lineament passes through the QZ (Rowly et al., 1978).

Cenozoic igneous activity in the Western U.S.

The igneous activity associated with the east-west mineral belts, seems to have migrated southward starting at 40 N., 43-34 m.y. ago moving to 37 N, 17-6 m.y. ago (Stewart et al., 1977). Armstrong et al. (1969) present a variation on this theme, with volcanism beginning about 40 m.y. ago in east central Nevada, migrating as a front outwards toward the margin of the Great Basin. One possible explanation proposed by the authors is that crustal fracturing began in the core area and slowly propagated outward, resulting in a slowly migrating volcanic front.

The general pattern of middle to late Cenozoic volcanism in the western U.S. was the eruption of Oligocene-Miocene intermediate volcanics (quartz latite-low silica rhyolite) followed by the eruption and emplacement of basalt and high silica rhyolite. This change in type of volcanism was coincident with the change from subduction related compressional tectonics to an extensional regime at the termination of subduction (Lipman et al., 1972; Christiansen and Lipman, 1972; Lipman et al., 1978). Eaton (1984) presents a more specific scenario in which 3 different periods of magma genesis are defined. The first is the emplacement of calc-alkaline andesites, rhyolite and quartz latite magmas during convergence-related compression. The second is the emplacement of high silica rhyolites, basaltic andesites and alkali basalts during intra-arc and back-arc spreading at rapid rates. The final stage, is marked by the emplacement of

tholeitic basaltic magma during reduced extensional rates. In the Basin and Range province, the change from intermediate to bimodal volcanism occurred in general between 22 and 24 m.y. ago.

This sequence and change in rock composition has been documented in the San Juan volcanic complex, the Thomas Range (Spor Mountain) and the Wah Wah Mountains (Lipman et al., 1976; Lipman et al., 1978; Lindsey, 1982; and Keith et al., 1986).

In these volcanic centers, particularly Spor Mountain and the San Juan volcanic system, significant mineralization (F, W, Be, and U, was associated with high silica alkalic rhyolites emplaced 5-15 m.y. after the end of the caldera cycle and coincident with the transition from compressional to extensional tectonics. The mineralization in the western San Juan mountains occurred in pulses from the most intense at 22.5 m.y. ago, to 15-17 m.y., and a final pulse at 11 m.y. ago (Lipman et al., 1976).

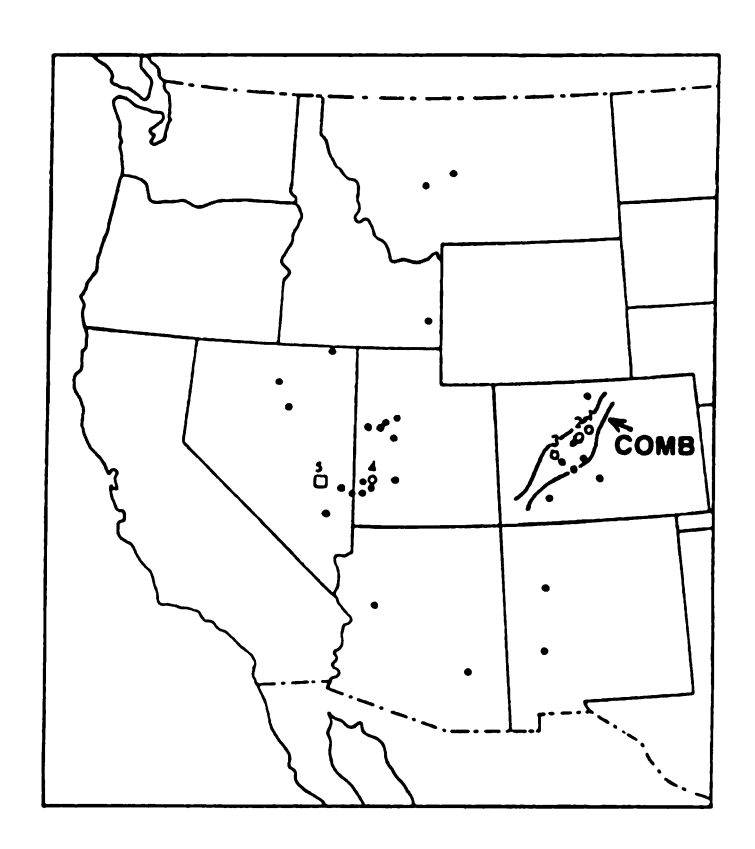
Both Oligocene and Miocene magmatism is evident in the southern Wah Wah Mountains, which host the Pine Grove intrusions and porphyry molybdenum deposit. Oligocene magmatism was characterized by dacitic ash flows and andesite lava flows. Miocene igneous activity is marked by a predominately bimodal assemblage of high silica rhyolite domes, dikes, ash flow tuffs and trachyandesite lava flows. The Pine Grove system is believed to have been formed 22-23 m.y. (Keith, 1980; Keith, 1982, and Keith et al., 1986).

Tertiary metallization in the Western U.S.

Several types of mineralization and metallization appear to be spatially and/or genetically related to the intrusion or extrusion of high-silica, fluorine-rich rhyolite magmas (topaz rhyolites). Among these are: 1) base and precious metal epithermal vein deposits (Ag, Au, Pb, Zn, W); 2) volcanogenic deposits of U, Be, F, Li, Sn and Cs; 3) fluorite breccia pipes, fracture fillings and as replacement bodies; 4) Climax-type porphyry deposits (Mo, W, Sn) and Mo-rich breccia pipies; and 5) pegmatites (Burt et al., 1982; Christiansen et al., 1983; Christiansen et al., 1986).

Many authors recognize that the magma types for these deposits are similar, possibly locally related, and were emplaced or extruded in a similar tectonic setting (Figure 11). There is evidence supporting similar magmas and magmatic processes in the genesis of these deposits (Burt et al., 1982; Christiansen et al., 1983; Christiansen et al., 1986). Hildreth (1979) demonstrates that Mo, Sn, W, Pb, Cs, Li, Be, F and U are enriched in the initial high-silica eruption of the Bishop Tuff.

From an exploration standpoint, the presence of base metal veining (particularly W, and Sn) and fluorite mineralization derived by high silica rhyolite porphyry intrusives may reflect a porphyry molybdenum deposit at depth (Burt et al., 1982; Christensen et al., 1986). The close spatial and temporal relationship between major fluorospar districts and Climax-type districts is widely recognized and accepted (Van Alstine, 1968; Lamarre and Hodder, 1978).



- TOPAZ RHYOLITES
- O URAD HENDERSON
- O CLIMAX
- O MT. EMMONS
- O PINE GROVE
- □ QUINN CANYON

Figure 11. Distribution of topaz rhyolites of the western U.S. relative to the location of the Quinn Canyon Range, the Pine Grove porphyry Mo system and the Urad-Henderson, Climax and Mt. Emmons porphyry Mo deposits of the Colorado Mineral Belt (COMB) (modified from Christiansen et al, 1986).

The genetic relationship between Au metallization and rhyolite porphyry intrusion is tenuous. It is possible that this magma type is not the main source for this metal, in many mineralized volcanic systems. This is supported by evidence that Au-quartz veins are sometimes found adjacent to quartz-latitic, andesitic, and rhyodacitic intrusives, and that Au, has been shown to be depleted in high silica magma chambers (Sainsbury and Kleinhampl, 1969; Hildreth, 1979; and Keith, 1980).

Based on limited Sr isotope data, Christiansen et al. (1986) believe that topaz rhyolites have a lower crustal source. Assuming approximate crustal province age, Christiansen et al. conclude that the Sr isotope ratios correspond to crustal source areas with relatively low Rb/Sr ratios. Citing the work of Pettingillet et al. (1984), Christiansen et al, suggest that a low Rb/Sr ratio is consistent with a granulite grade source. The broad distribution of topaz rhyolites in the western U.S. suggests that there probably is significant variability in source material (Figure 11).

Stewart et al (1977) define two major metallogenic provinces in the Western U.S. The western province, characterized by precious metals, antimony, arsenic, and mercury, is delineated by a north-south trending line, parallel to and 100km west of the western boundary of the Quiet Zone. This line is roughly coincident with the western edge of the Precambrian craton as positioned by Farmer and Depaolo (1983) and the appearance of transitional assemblage

sedimentary rocks. The eastern metallogenic province is characterized by base-metal and lithophile element mineralization.

CLIMAX-TYPE PORPHYRY MOLYBDENUM DEPOSITS

The Climax-type porphyry molybdenum deposits are a specific variety of stockwork molybdenum deposits, which are confined in terms of geologic setting and time of emplacement. These deposits have produced over half of the worlds production of molybdenum, with the mine at Climax, Colorado, being the worlds single largest producer of molybdenum (Westra and Keith, 1981; and White et al., 1981).

Climax-type porphyry molybdenum deposits are characterized by the style and intensity of mineralization and alteration, age and petrochemistry of the associated granitic plutons.

Deposits discovered to data include Climax, Urad-Henderson, Mt. Emmons-Redwell Basin, and Pine Grove (Wallace et al., 1978; White et al., 1981; and Westra and Keith, 1981). With the exception of Pine Grove (Utah), the Climax type deposits are confined to the Colorado Mineral Belt (Figure 11), a northeast-trending, mineralized shear zone cutting across western Colorado (Tweto and Sims, 1963). Pine Grove has been classified as a Climax-type deposit, although some authors have expressed a degree of uncertainty (Keith et al, 1986).

Volumes of material have been published on the Climax-type systems. Westra and Keith (1981) propose a classification scheme for stockwork porphyry molybdenum deposits, based on their magma series chemistry, focusing on the characteristics and origin of the Climax-type. Mutschler et al (1981) present

a different classificiation system for stockwork molybdenum deposits based on pluton chemistry and age. A detailed description of Climax and Urad-Henderson is presented by Wallace et al. (1968) and Wallace et al (1978), respectively. White et al. (1981) describe the important features of Climax-type deposits and the possible origin of magmas and metals. These publications represent fairly exhaustive studies of the ore-forming systems, but are a small fraction of the published and unpublished studies.

The following section is a brief overview of the Climax-type deposits, specifically the petrochemical signature of the source rocks, mineralization, alteration, emplacement history, and the origin of the granitic intrusives and metals.

Geology

Mount Emmons-Redwell is generated by granitic and rhyolitic porphyry stocks. These stocks range in size from 1600 ft-4500 ft in diameter and were emplaced between 33 and 17 m.y. ago, during crustal relaxation, coincident with and following initiation of the Rio Grande Rift (White et al., 1981; Westra and Keith, 1981; Stein, 1985 and Christiansen et al., 1986).

A key feature of these districts is the multiple intrusion of magmas. At Climax, this results in stacked, umbrella-shaped ore shells, which cap and correspond to hydrothermal activity associated with successive pulses of granitic magma. The ore is distributed in

quartz - molybdenite veinlets in the ore zone and the ore forming solutions appear to have exsolved directly from the crystallizing magma (Wallace et al., 1968; Wallace et al., 1978; Mutschler et al., 1981; White et al., 1981; and Westra and Keith., 1981). Ore grades range from .2% to 1.0%, with averages between .3% and .45% (White et al., 1981; Edwards and Atkinson, 1986).

Unlike Pine Grove, the deposits at Climax and
Urad-Henderson appear to have no associated comagnatic
eruptive volcanic units. It should be noted, however, that
they do occur in deeply eroded terranes, in part caused by
large-scale post-ore movement along major regional faults. By
reconstructing the Paleozoic section above the deposit, the
upper ore body at Climax was formed between 6,600 and 9,600 ft
below the surface. Molybdenum metallization at
Urad-Henderson, occurred at depths of 2,500-3,400 ft and
5,700-7,500 ft respectively (White et al, 1981). The Pine
Grove vent is believed to be eroded 1.7 km below the
pre-eruption surface (Keith, 1980; Keith, 1982; Keith et al.,
1986).

Mineralogy and alteration

Four main types of alteration zones are found above and peripheral to the ore bodies and plutons. In order from inner to outer, they are; the potassic zone, the quartz-sericite-pyrite zone (phyllic zone), an upper and lower argillic zone and a propyllitic zone (dominated by chlorite,

clay, epidote, and calcite) Wallace et al., 1968; Lowell and Guilbert, 1970, Mutschler et al., 1981; White et al., 1981; and Westra and Keith, 1981).

Tin, tungsten and base metal halos frequently develop above, or in the case of tungsten, can coincide with the molybdenite ore body. Huebnerite, wolframite and less commonly scheelite are the principal tungsten-bearing minerals. Cassiterite has been recognized by Wallace et al (1968), with its crystallization synchronous with tungsten mineralization. Fluorite, and to a lesser degree, topaz, are found in veins in the phyllic zone and the potassic zone. The highest fluorine concentrations are found directly above the ore zone. Paragenetically late lead, zinc, silver and to a lesser degree copper, are deposited in zones well above the ore bodies and adjacent to late rhyolite dikes (Westra and Keith, 1981; White et al., 1981). Copper minerals are rare, with a high Mo/Cu being a prominent feature of the deposits.

Petrochemistry of granitic rocks

The igneous rocks associated with Climax-type Mo deposits are highly differentiated peraluminous-metaluminous granites and rhyolites. They are characterized by high SiO2, and K2O (with K2O>Na2O) and low MgO, TiO2, CaO and Fe.

The trace element signature is defined by an enrichment of Rb, Nb, F, Mo, W, Th, Sn, and U, and a depletion in Ba and Sr (Westra and Keith, 1981; and White et al., 1981). Although the granitic rocks display these general characteristics,

there is a variation in the range of trace element values between districts. The typical trace element ranges, as defined by Westra and Keith (1981), are; 200-800 ppm Rb (with isolated values exceeding 1000 ppm), 25 to greater than 250 ppm Nb, generally less than 100 ppm Sr (frequently less than 20 ppm), less than 150 ppm Ba, and less than .2% TiO2. Values for the Climax district and nearby Urad-Henderson tend toward the extremes of the ranges, with values of less than 10 ppm Sr and less than 80 ppm Ba common.

Published REE data is virtually nonexistent, but Stein (1985) states that REE patterns display relatively large negative europium anomalies. Analyses from this study, also show significant Eu anomalies and a La/Ybn ratio of about 6. Detailed petrochemical comparisons with the Quinn Canyon high silica rhyolites follows in a later chapter.

Origin of granitic rocks

Two main theories have been proposed for the origin of Climax-type granites and rhyolites. The first, supported by Westra and Keith (1981), Lamarre and Hodder (1978) and Van Alstine (1976), is a mantle source for the magmas and molybdenum. The second theory precludes a mantle source and suggests a middle and/or lower crustal source for the magmas. This theory, based on isotopic evidence, has found wide support among various workers, such as White et al. (1981), Farmer and DePaolo (1984), Lipman et al. (1978), Zartman (1974) and Stein (1985).

Westra and Keith (1981) propose that melting of the upper mantle above a subducting slab produced alkali-calcic magmas enriched in volatiles, such as F, and incompatible elements. The release of F-bearing hydrous fluids was caused by the dehydration of phologopite in the subducted slab at depths greater than 250 km. This hydrous fluid would initiate partial melting of mantle peridotite. The resultant melt would be highly enriched in K, F and other incompatible elements. Mo and Sn, the authors suggest, would be added as the melt was introduced into the upper mantle.

Work by Zartman (1974) and more recently Farmer and DePaolo (1984) and Stein (1985) utilizes Pb, Nd, and Sr isotopes in defining a probable source for Climax-type deposits, particularly in the Colorado Mineral Belt.

Molybdenum deposits of the Colorado Mineral Belt fall into Area I of Zartman's (1974) lead isotope classification system for the Western U.S. In this province, igneous rocks and ore samples displayed a considerable range in lead isotope composition, but were generally indicative of a lower crustal source or possibly upper mantle.

Several conclusions were reached by Farmer and DePaolo (1984), among these were: 1) Cu-mineralized granites in general have a mantle source, 2) Climax-type Mo-mineralized granites have a crustal source, with a mantle component being highly unlikely, and 3) the granites at Henderson appear to have a Rb-rich middle crustal source, because of their high

€ sr. The authors propose that this high € sr may be a result of contamination by radiogenic Sr derived during hydrothermal alteration of the nearby Silver Plume Granite.

Stein (1985) suggests based on Pb and Sr isotope data, that the Climax-type granites have a 1.4 b.y. lower crustal source, which had previously undergone granulite facies metamorphism. This source material probably had a low U/Pb ratio, but a close to average Th/Pb ratio. Stein states that Climax-type granites cannot be simple mantle melts. Likewise, a mantle source contaminated by upper crustal material or a purely upper crustal source seems implausible. Stein concludes that Climax-type granites are not differentiates of or genetically related to the source material producing the older intermediate intrusives in the Colorado Mineral Belt. The author further proposes that this apparent difference in source material may be due to "localized" or "specialized" partial melting of a lower crust material during the change from compressional to extensional tectonics (p. 271).

DISCUSSION AND RESULTS

Quinn Canyon Silicic Rocks

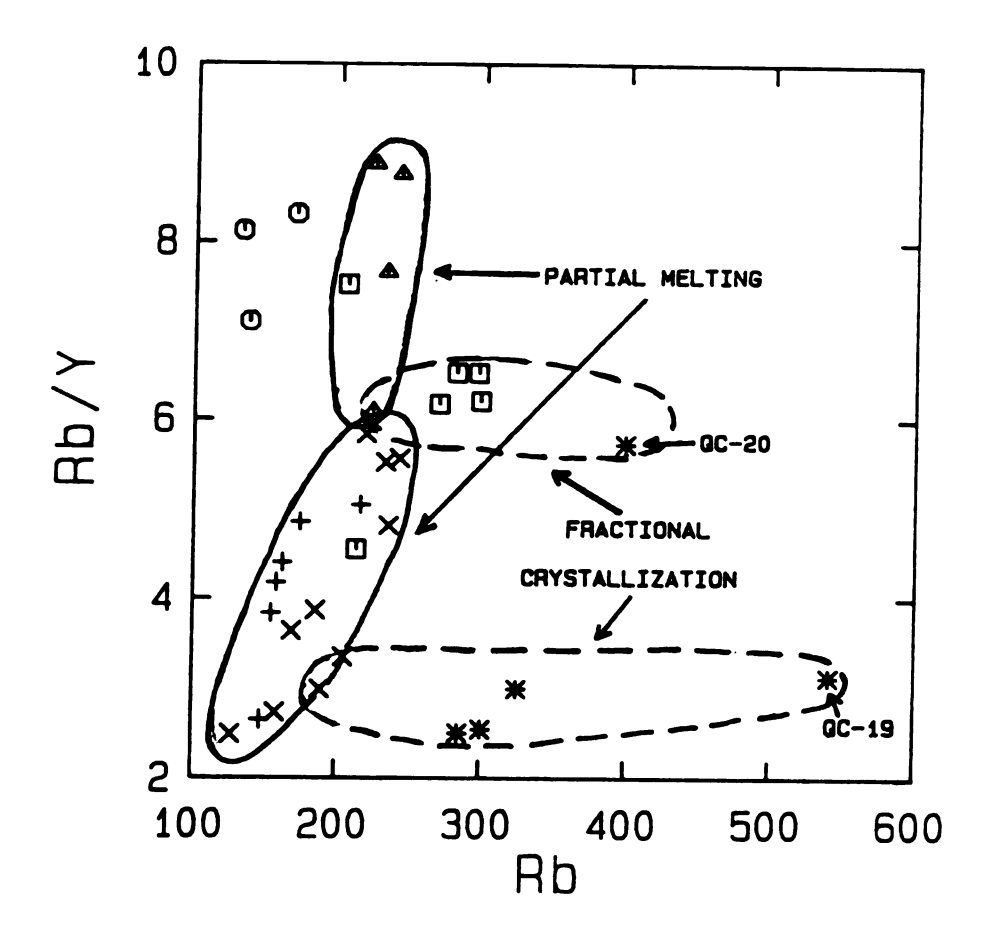
Several groups have been delineated according to trace element chemistry and to a lessor extent, petrography.

Although a quantitative and unequivocable determination of the relationship among these groups or individual rocks is not attempted in this study, some meaningful conclusions have been reached.

Although not definitive, some variation diagrams, including a process identification diagram (see Minster and Allegre (1978) and Allegre and Minster (1978) for explanation) of Rb/Y vs Rb, suggests that the rhyodacite dome samples are not cogenetic with the other rhyolitic hypabyssal samples (Figure 12).

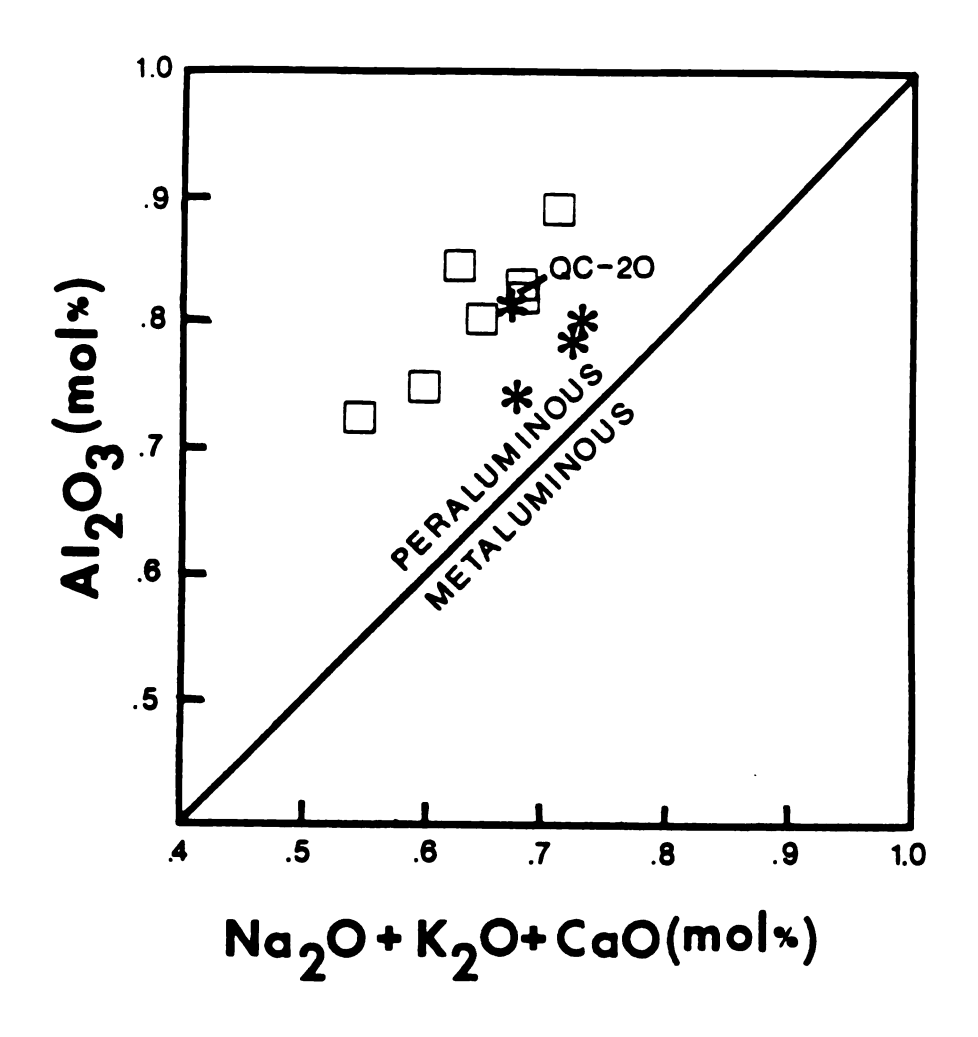
The group of rhyolites displaying the most extreme enrichment in the incompatible elements (Nb, Y, Th and Rb) appear to have a different source than the muscovite-bearing rhyolite samples (group 1). The strength of this comparison is that both "groups" have at least some characteristics of being highly differentiated, particularly in terms of the depletion in Ba, Zr, La, Ti, and Eu. The lines of evidence supporting a different source are:

1) The muscovite-bearing rhyolites are more peraluminous (Figure 13).



- O RHYODACITES
- + LOW SILICA RHYOLITES
- × RHYOLITES
- ▲ MUSCOVITE-BEARING RHYOLITES 2
- MUSCOVITE-BEARING RHYOLITES 1
- *** INCOMP. ELEMENT-RICH RHYOLITES**

Figure 12. Plot of Rb/Y vs Rb indicating possible partial melting (solid lines) and fractional crystallization (dashed lines) trends for the Quinn Canyon silicic rocks.



- * INCOMPATIBLE ELEMENT-RICH RHYOLITES
- MUSCOVITE-BEARING RHYOLITES GROUP 1

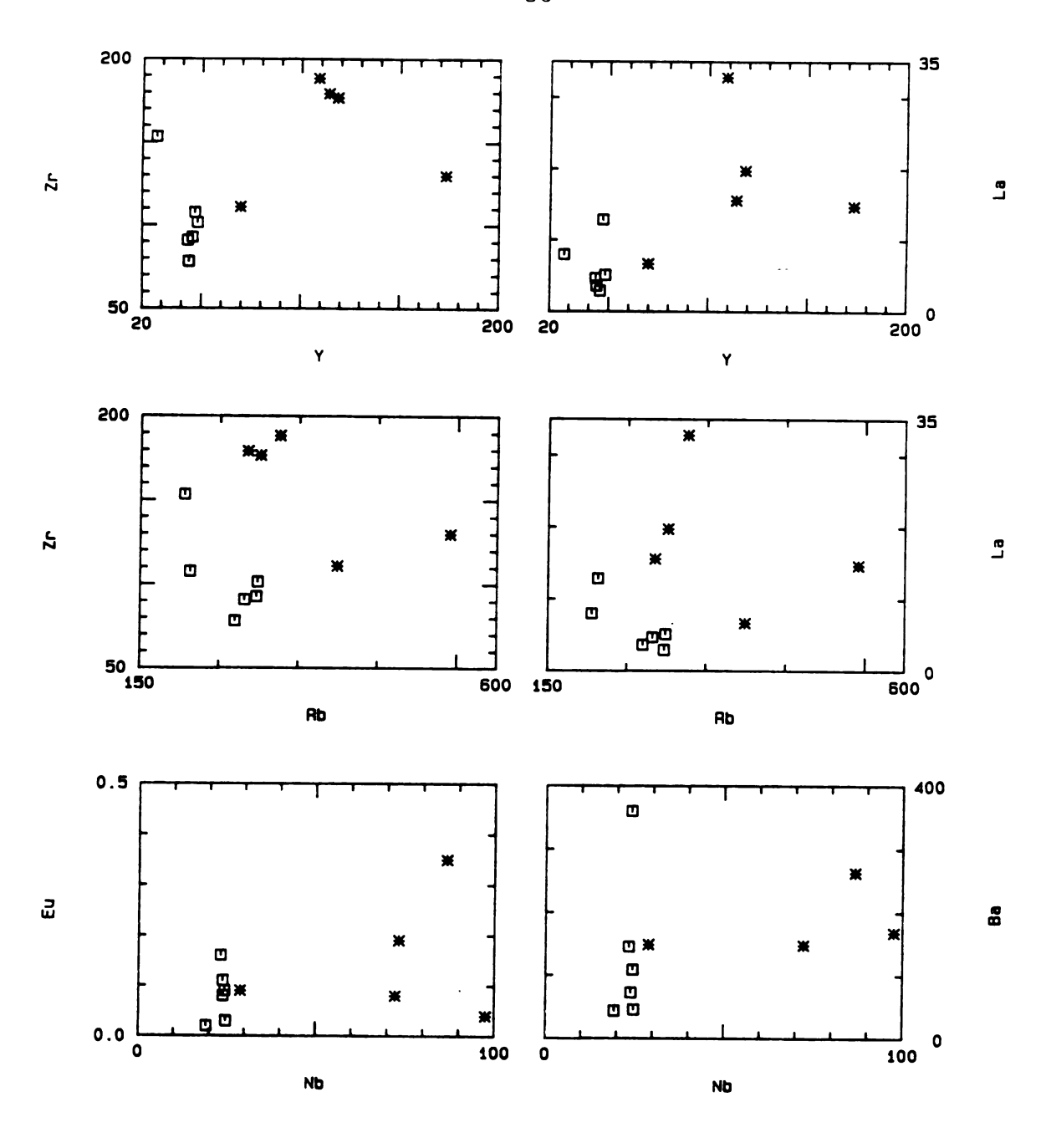
Figure 13. Plot of molecular Al2O3 vs molecular Na2O+K2O+CaO for the incompatible element-rich rhyolites and muscovite-bearing rhyolites (group 1). Sample QC-13 has not been included because of alteration affecting NaO.

2) The muscovite-bearing rhyolites appear highly differentiated, being equally or more depleted in Eu, Zr, Ti, Ba, and LREE, yet are only minimally enriched in Th, Nb, Y and Rb, when compared to samples Qc-19, Qc-19c, Qc-13 and Qc9-3 (Figure 14).

It may be possible to explain the trace element composition of the muscovite-bearing rhyolites by invoking a similar source which has undergone a previous partial melting event. It is more likely, however, considering one group is more peraluminous, that they are not cogenetic.

Fluorine-rich rhyolites, such as topaz rhyolites, are generally classified as A-type or anorogenic granitiods, and are believed to be produced by the partial melting of a lower crustal source (Burt et al., 1982; Christiansen et al., 1983; Christiansen et al., 1986). The muscovite-bearing rhyolite group 1, relative to the incompatible element-rich rhyolites at Quinn Canyon have a trace element signature more similar to that of S-type granites. These characteristics are a depletion in Ba, Rb, Zr, Y, Ce and Nb and an enrichment in Sr, compared to A-type granites (White and Chappell, 1983). Although the muscovite-bearing rhyolites may not be the high-level equivalent of "pure" S-type granites, they seem to have many of the trace element compositional features.

Farmer and Depaolo (1984) indicate that peraluminous granites (such as S-type) may be derived from a midcrustal source (p 10,151). Farmer and Depaolo (1983) state that the compositional differences seen in miogeoclinal granites of the Eastern Great Basin may be due to the assimilation of various



□ MUSCOVITE-BEARING RHYOLITES 1

※ INCOMP. ELEMENT-RICH RHYOLITES

Figure 14. Plots of Ba and Eu vs Nb, La and Zr vs Rb, and La and Zr vs Y for the incompatible element-rich rhyolites and muscovite-bearing rhyolites (group 1).

amounts of pelitic sedimentary material, with the magma body. This suggests that the muscovite-bearing rhyolites of Quinn Canyon may have a source higher in the crust than that assumed for the incompatible element-rich rhyolites of this suite, or may be the result of the mixing of upper crustal pelitic sedimentary material with the parent magma.

Sr, Nd and/or Pb isotope values are needed to accurately constrain the source material of the silicic rocks, both locally and for regional comparisons.

Both groups of rhyolites are probably a result of some degree of crystal fractionation from a parent formed by small amounts of partial melting. Samples Qc-20, Qc-19C, Qc-13, and Qc9-3 (incompatible element-rich rhyolite group) are the result of large degrees of fractionation from a more "primitive" rhyolite as suggested by Christiansen et al. (1986). The less evolved, "rhyolite group" probably is genetically related to and possibly the "parent" of one or many of the incompatible element-rich rhyolites. This conclusion is supported by some process identification diagrams, including a plot of Rb/Y vs Rb (Figure 12).

The extreme enrichment in incompatible elements evident in sample Qc-19, may indicate that it has been the most fractionated, and/or possibly is not genetically related to other members of its "group".

Qc-20 has enrichment trends which "fall" between the two groups, but is distinctly peraluminous, indicating that it may have been derived from a source similar to that which generated the muscovite-bearing rhyolites (group 1), and/or

perhaps is directly related by fractional crystalization.

Petrochemical Comparisons

The focus of this comparison is on trace element composition. Specifically, the enrichment in the incompatible elements that are characteristic of the granitic and rhyolitic rocks which generate porphyry Mo, Sn, and W, and lithophile-type (F, Be, Li, and U) mineralization. This petrochemical signature is marked by an enrichment in Nb, Y, Th, and Rb and depletion in Sr, Ba, Zr, and Eu. Major element chemistry is similar for most F-rich rhyolites and granites, and alone, is not adequate for comparison of magma chemistry, relative to the potential for generating the metallization and mineralization mentioned above.

Analyses of samples from Urad-Henderson (8), Mount Emmons (1) and Pine Grove (3) form the basis of this comparison, supplemented by data taken from published and unpublished studies. The arthimetic mean of selected trace element concentrations are presented in Table 3. Major and trace element compositions of all samples are available in Appendix A.

Most of the Quinn Canyon (QC) rhyolites are much less enriched in the key incompatible elements, even comparing samples with equivalent SiO2. Because the source rocks of Climax-type deposits and other F-rich rhyolites represent extreme differentiates, only the high-silica incompatible element-rich and relatively unaltered samples are considered

Table 3. Arthimetic mean of selected trace elements for the Climax-type rhyolites and the Quinn Canyon incompatible element-rich rhyolites.

			CLIMAX-TYPE RHYOLITES	RHYOLITES		QUINN
	Climax (Stein, 1985) (2)	Urad-Henderson (8)	Mt. Emmons (1)	Pine Grove (Keith, 1982) (3)	Pine Grove (3)	Incompatible Element-Rich Rhyolites (5)
Ba	42	109	100	115	111	169
R P	652	554	321	364	427	370
£	115	91	80	37	46	72
<u>.</u>	I	48	28	16	13	18
డ	25	14	19	35	17	18
Ev	i	Е:	4.	80.	4.	21.
Sm	i	7.1	9.5	8.5	8.2	11
Z	19	112	209	68	75	157
TiO2	.05	.12	.2	9.	.02	29.
>	39	79	36	66	93	117
χρ	1	4.5	.3.3	6.5	4.1	6.4

in detail. The members of this group are not necessarily genetically related.

"Enrichment factor diagrams" of this group (Qc-13, Qc-19, Qc-19c, Qc-20, Qc9-3) divided by the mean of the Pine Grove, Urad-Henderson and Mt. Emmons samples illustrates the relative enrichment trends (Figure 15).

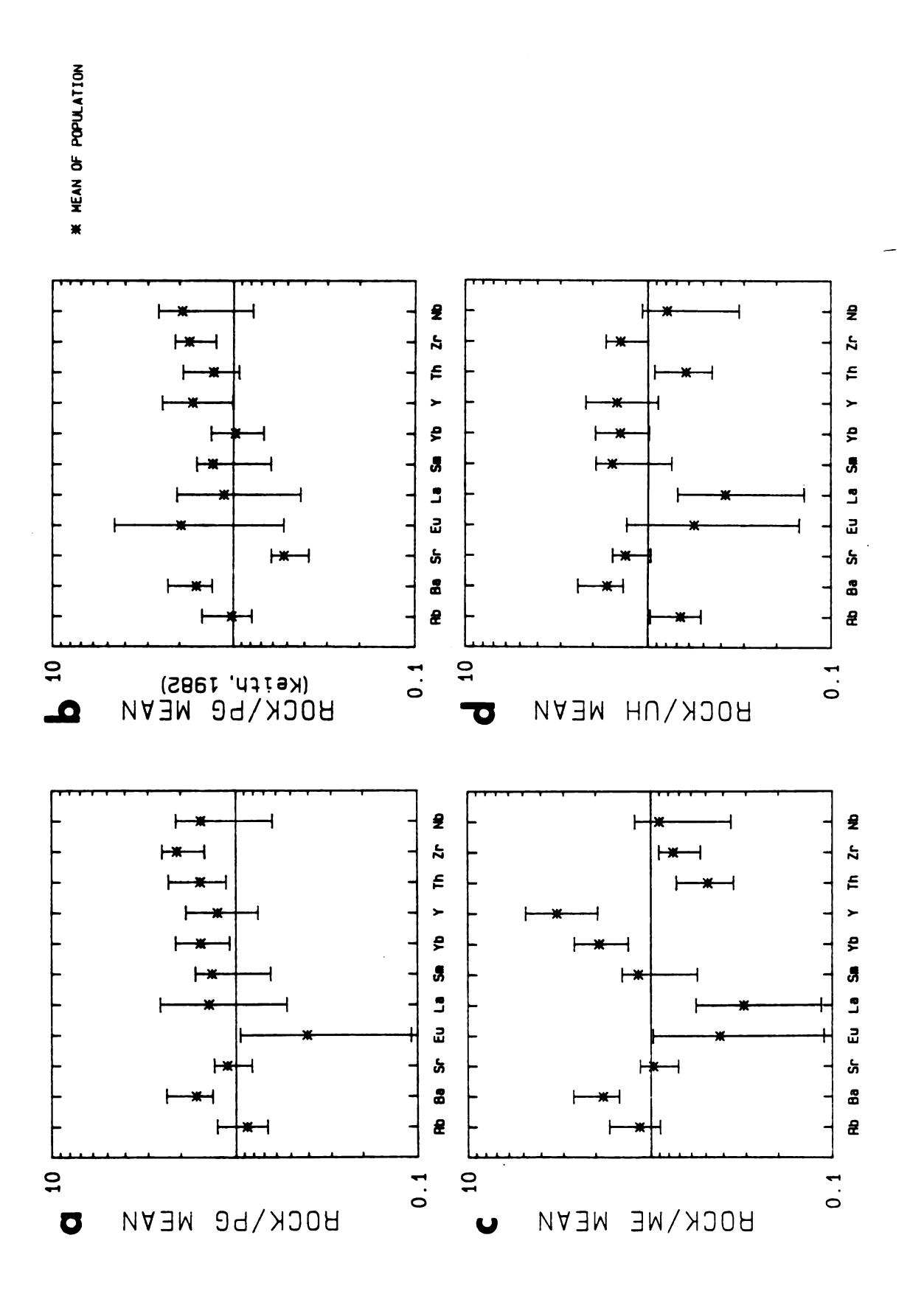
Overall, the trace element composition of the QC rhyolites is more similar to the Pine Grove rhyolites, than to the Urad-Henderson and Mount Emmons granitic rocks (traditional "Climax-type" source rocks). This is particularly evident when examining Rb values and REE distribution. Compared to Urad-Henderson, the QC rhyolites are less enriched in Rb, Nb, and Th and less depleted in Sr and Ba. They are, however, more enriched in HREE and depleted in LREE, resulting in a much more "flat" REE distribution pattern and display a greater negative Eu anomaly (La/YbN average of 6 for Urad-Henderson and 1.5 for QC) (Figure 16). Y, behaving in a similar manner as the HREE, is enriched in the QC rhyolites, and Ti depleted (Figure 15).

Published data from the Climax Mine, Henderson and Urad, support the trace element differences noted previously.

Samples from the Climax Bartlett and Wallace Stock and Late Rhyolite dikes have Rb>600 ppm, Sr<40 ppm, Nb>100 ppm, and Y values from 38-42 ppm (Stein, 1985).

Examination of the one Mount Emmons analysis from this study shows a lower Rb and Y value than Urad-Henderson or Climax, but a similar REE distribution pattern (Figure 16). Similar Rb, Y, REE and other key element values for the Mount

element-rich rhyolites normalized to the mean of selected trace elements of rhyolites and granites from: a) Pine Grove (PG; this study), b) Pine Grove (PG; Keith, 1982), c) Mount Emmons (ME) and d) Urad-Henderson (UH). The ranges of values for the Quinn Canyon rhyolites are shown by vertical Enrichment factor diagram of the Quinn Canyon incompatible Figure 15. bars.



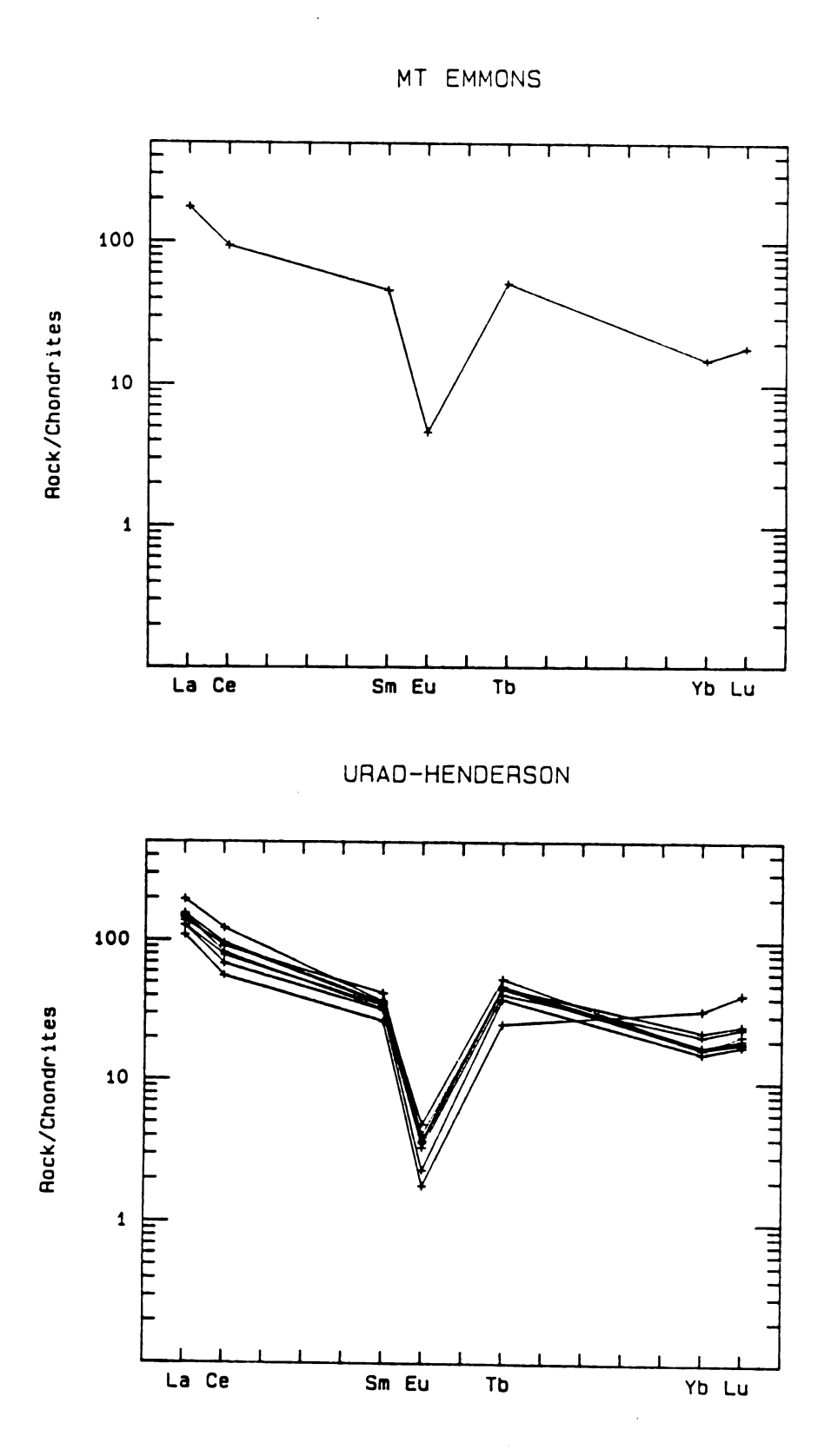


Figure 16. Chondrite-normalized REE patterns for Mt. Emmons and Urad-Henderson samples.

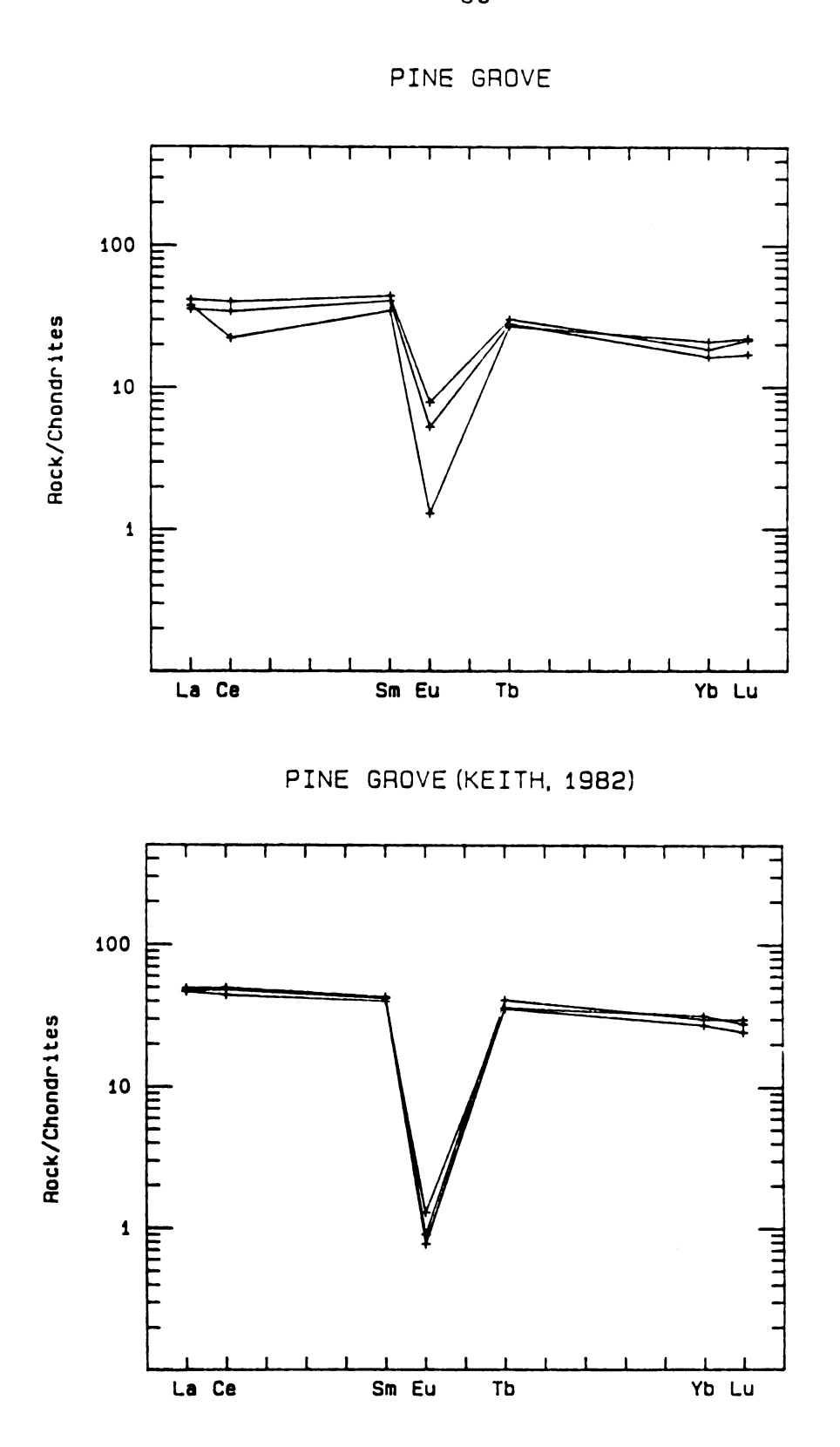


Figure 17. Chondrite-normalized REE patterns for rhyolites of Pine Grove (this study) and Pine Grove (Keith, 1982).

Emmons Keystone Porphyry and Redwell Pipe, are listed by Stein (1985).

Two sets of Pine Grove (PG) data are used for comparison.

The first set is from a group of undivided surface samples and samples taken at depth, analyzed at Michigan State

University. The second group consists of the average of analyses of one sample each of the Pine Grove Porphyry, Phase Five Porphyry, and Phase Four Porphyry (Keith, 1982).

The QC rhyolites are moderately enriched in Nb, Th, Zr, Y, somewhat depleted in Rb and have similar La/YbN ratios (1.5-2.0), to those of Pine Grove (PG). Eu and Sr values differ considerably between the two sets of PG data, with the analyses from Keith (1982) displaying larger Eu depletions and higher Sr concentrations (Figures 15 and 17).

The intrusive Pine Grove Porphyry has a Mo concentration of 4 ppm and Sn concentration of 8 ppm (Keith, 1982), compared to 3 ppm and 15 ppm respectively, for the most enriched QC rhyolite dikes. The mineralized Phase Four and Five Porphyry at Pine Grove have Mo concentrations ranging from 65-150 ppm.

The low La/Ybw displayed by the most evolved QC and PG rhyolites are common among F-rich rhyolites such as topaz rhyolites. Topax rhyolites as defined by Christiansen et al. (1986), typically have La/Ybw ratios of 1 to 3, are enriched in the incompatible lithophile elements (Rb, U, Th, Ta, Nb, Y, Be, Li, and Cs) and depleted in Sr, Eu, Ba, Ti, Zr, and Hf. Fluorine concentrations range from less than .2 to more than 1.0 wt%. F/C1 ratios are high (Christiansen et al., 1986). Although topaz has not been observed in thin section, fluorite

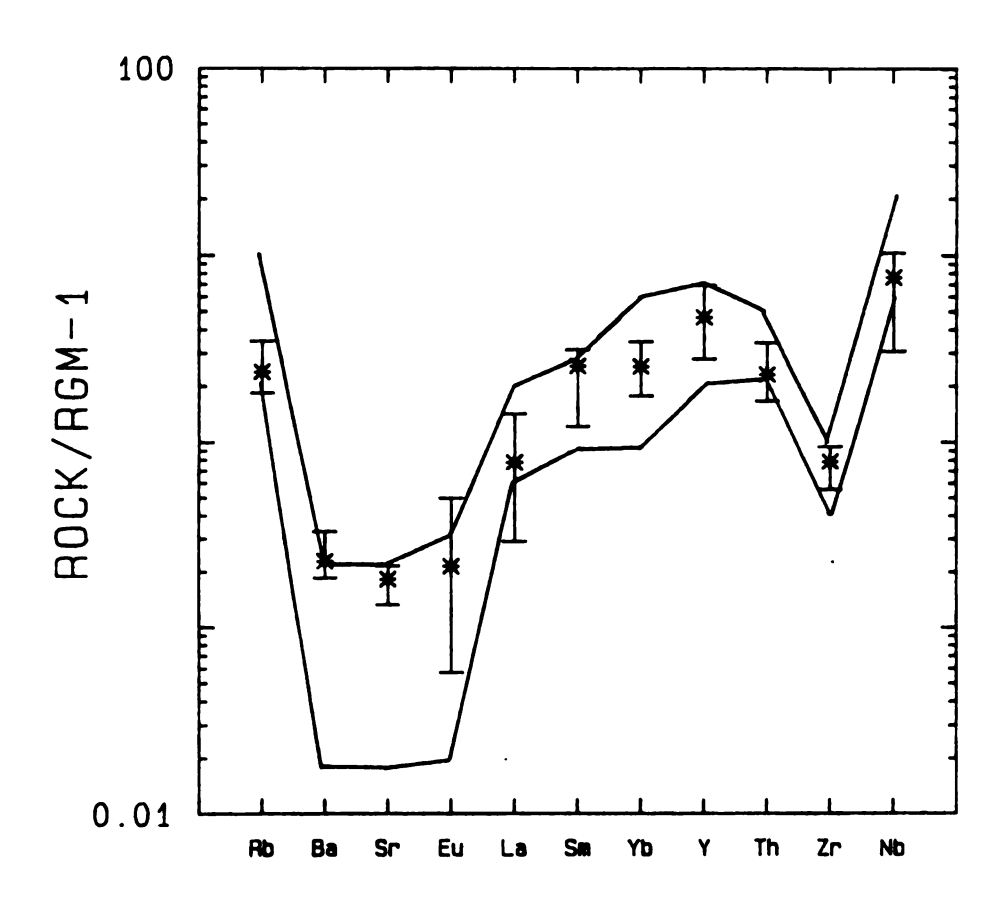
is present in some of the QC rhyolites and many key elements for most samples fall within the range published by Christiansen et al (1986) for topaz rhyolites of the western U.S. (Figure 18). It must be emphasized that the mean values of the elements Rb, Ba, Sr, and Th, barely lie within topaz element ranges.

Pb, Mo, and Sn data for topaz rhyolites is limited, but in general, these elements occur in higher concentrations than the few analyzed samples from QC. It is important to note that the analysis of these elements and F (Christiansen et al., 1986) are from vitrophyres. Devitrification and/or the release of magmatic fluids from the QC intrusives would probably result in a lowering of these element levels, certainly at least volatiles such as F.

Christiansen et al state that although the Pine Grove rhyolite tuff lies within the range of all topaz rhyolite compositions, relative to topaz rhyolites in SW Utah, it is enriched in Ba, Sr, Sc, and A1 and depleted in F, Zr, Rb, Nb, Ta, Th, U, Yb, Y and Mo. The authors imply that the 22-23 m.y. rhyolites at Pine Grove are not considered "true" topaz rhyolites, because of their only marginally qualifying geochemical signature.

Source material comparison: isotopic evidence

The Quinn Canyon Range is not only geographically close to the Pine Grove volcanic system but has a similar age of rhyolite emplacement (23 m.y. for Quinn Canyon, and 22-23 m.y.



* MEAN OF POPULATION

Figure 18. Range of values of selected trace elements for topaz rhyolites of the western U.S. compared to the Quinn Canyon incompatible element-rich rhyolites. All values normalized to U.S.G.S. standard RGM-1. Vertical bars represent ranges of concentrations for the Quinn Canyon incompatible element-rich rhyolites (after Christiansen et al., 1986).

for Pine Grove; Keith, 1982; Keith et al., 1986), a similar general geologic setting and is located along the same mineralized lineament. Based on these similarities, it is not surprising that the Miocene rhyolite flows and intrusives of the Pine Grove area are compositionally closer to the Quinn Canyon rhyolites, than the granitoid porphyries associated with more traditional Climax-type deposits located in the Colorado Mineral Belt.

Major differences in rhyolite trace element composition and associated metalization may be attributed to a difference in source material. As mentioned earlier, Climax-type granitic source rocks are believed to have a lower crustal source, which has undergone granulite facies metamorphism (Zartman, 1974; White et al., 1981; Farmer and Depaolo, 1984; Stein, 1985; and Christiansen et al., 1986).

Sr and Nd isotope data are not presently available for the Pine Grove deposit. Pine Grove is located at the boundary of the Rb-depleted lower crust (granulite facies metamorphism) of the western carton, as delineated by Farmer and Depaolo (1983) (Figure 19). This limit is based on a discontinuity in granite Sr isotope composition, obtained from samples taken across the northern Great Basin and from Tertiary granites of Colorado. Low &sr values are interpreted as being derived from a granulite-grade lower crust, while higher &sr values of the miogeocline to the west are suggestive of a basement with no "depleted" lower crust. A second discontinuity in &wa and &sr to the east marks the basement edge. The Quinn Canyon Range is located significantly west of the

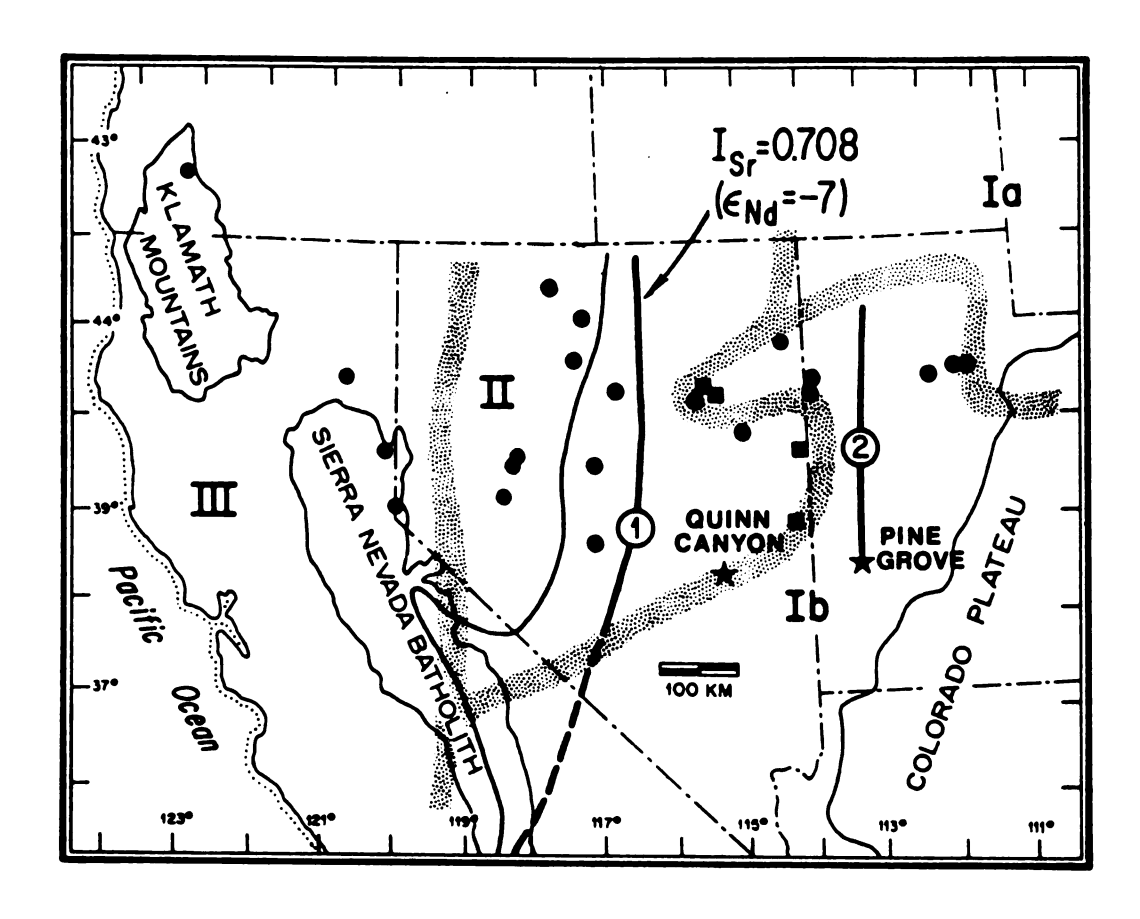


Figure 19. Map showing the intrepreted western limit of Precambrian basement (line 1) and western limit of a granulite grade lower crust (line 2) (Farmer and Depaolo, 1983). Pb isotopic provinces from Zartman (1974) are defined by stipled bands and identified by Roman numerals. See text for further explanation (modified from Farmer and Depaolo, 1983).

granulite facies line (Figure 19), in the area of "non-depleted" lower basement.

Four Pb isotope provinces (Ia, Ib, II, III) are defined by Zartman (1974) for the western U.S., with each province reflecting a somewhat specific source material. Climax-type deposits all occur in area Ib, characterized by a fairly unradiogenic Pb206/Pb204 ratio of 16.2-18.8, a Pb208/Pb204 of 36.5-39.9, and a basement rock age of 1.8 b.y. The Quinn Canyon Range lies in a transition area between area Ib and area II, characterized by a more radiogenic Pb isotope composition $(Pb^{206}/Pb^{204}=19.1-19.7,$ Pb208/Pb204=38.9-40.3) (Figure 19). According to Zartman, a Pb206/Pb204 ratio of 18.8 is the most important factor separating region Ib and II. The placement of this boundary relative to the Quinn Canyon Range is based on a Pb isotope values from galena sample taken from a vein adjacent to a dacite dike (Pb206/Pb204=18.886, Pb207/Pb204=15.640, Pb208/Pb204=39.077; Zartman, 1984). Pine Grove also lies within region Ib, but very close to the II boundary (Figure 19). A galena sample taken from the southern Wah Wah mountains, Utah (probably from the Pine Grove system) has a Pb isotope signature similar to the Quinn Canyon transitional Pb isotope signature (Pb206/Pb204=18.921, $Pb^{207}/Pb^{204}=15.780$, $Pb^{208}/Pb^{204}=39.988$) (Stacey et

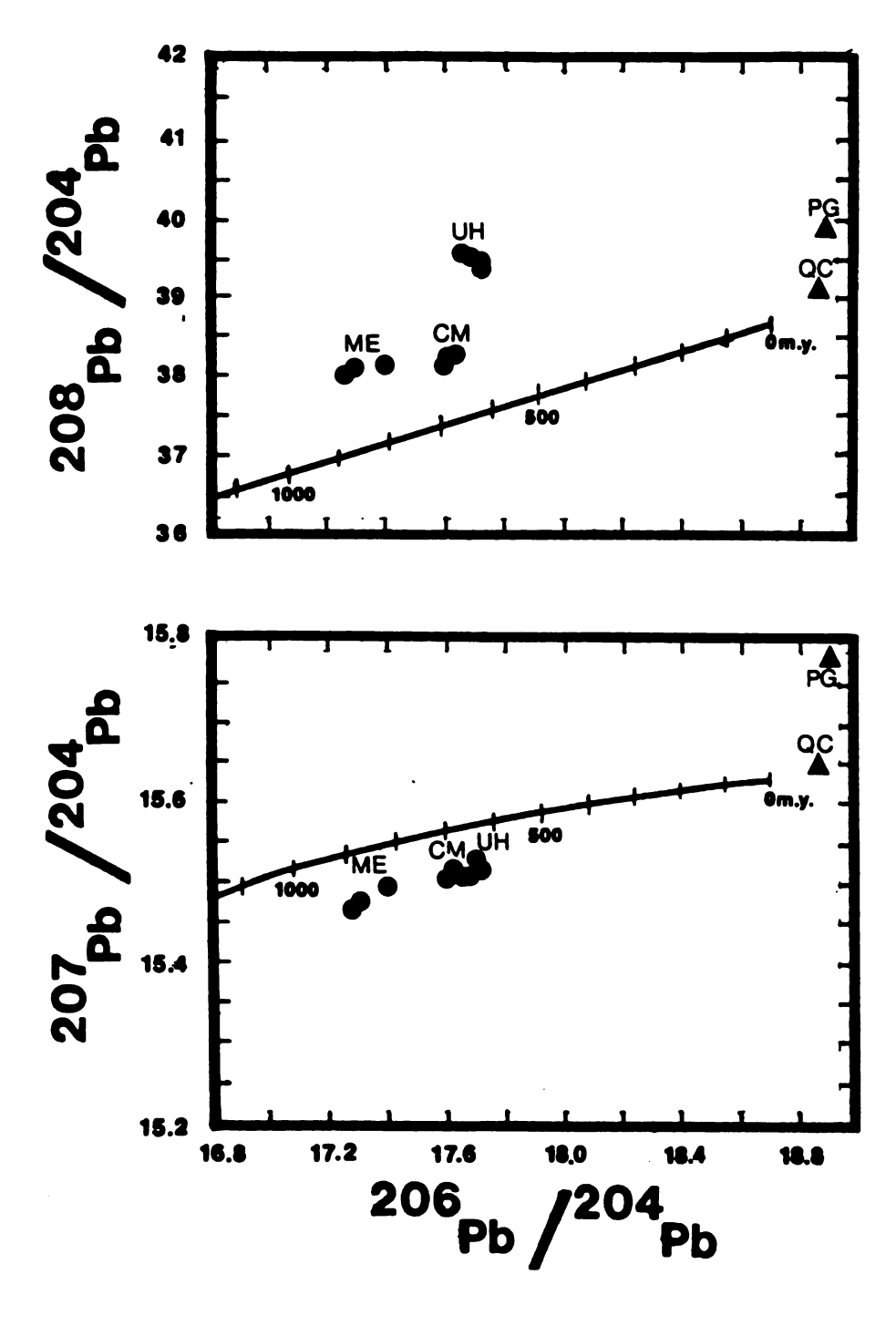
Doe and Zartman (1979) state that Mesozoic and Cenozic igneous rocks of region II, could be generated from the partial melting of either upper crustal miogeosynclinal rocks

al., 1968).

or from a non-cratonized Precambrian source (never metamorphosed above amphibolite facies). The Pb isotopic signature of these materials are not easily differentiated and would exhibit a similar relationship to the Pb isotopic signature of granulite facies lower crustal source materials.

Stein studied Pb and Sr isotope data from the Colorado Mineral Belt and concluded that even within a somewhat restricted region, Pb isotope composition was significantly different among Laramide-Tertiary granites. These small yet significant variations Stein attributed to subtle differences in age and composition of source materials. Stein also recognized that granitiods associated with major molybdenum mineralization had noticeably less radiogenic Pb206 and Pb207 isotopes, compared to barren granitiods.

Paired Pb-Pb diagrams indicate that Urad-Henderson,
Climax and Mount Emmons have considerably less radiogenic
Pb208 and Pb207 and somewhat similar Pb208 isotope
values than those of Quinn Canyon and the southern Wah Wah
mountains (Pine Grove). The data from Pine Grove and Quinn
Canyon plot above the average Pb growth curve of Stacey and
Kramer (1975) for both Pb207 and Pb208 vs Pb208, while
those from Climax, Urad-Henderson and Mount Emmons plot below
the Pb207 curve and above the Pb208 curve (Figure 20).
This relationship may suggest that the source area of the
traditional Climax-type granitiods had a higher Th/U ratio.
The apparent depletion of U relative to Th and Pb, in the
source material of the Climax-type granitiods, has been
compelling evidence for a granulite-grade lower crustal source



● Pb-K FELDSPAR

▲ Pb-GALENA

Figure 20. Lead isotope data for Pine Grove (PG), Quinn Canyon (QC), Urad-Henderson (UH), Mount Emmons (ME) and Climax (CM). The lead growth curves are from Stacey and Kramer (1975). Data from Zartman (1974), Stacey et al. (1968) and Stein (1985) (after Stein, 1985).

(see Stein, 1985 for further discussion).

Although detailed Pb and Sr isotope study is needed at Quinn Canyon and Pine Grove, limited data suggests that both of these Miocene igneous and mineralized systems may be the result of partial melting of a non-depleted or non-cratonized source, or at least an appreciably different source material than that which gave rise to granitiods genetically related to metallization at Urad-Henderson, Climax, and Mount Emmons. The implication of Stein's work is that a specific source material is necessary for the development of economic-grade molybdenum mineralization. There appears to be a direct correlation between the amount of radiogenic Pb isotopes, enrichment in incompatibles (particularly Rb) and associated "economic" potential for molybdenum mineralization.

The Pine Grove system is enigmatic in terms of trace element chemistry, and tentatively, Pb isotopic signature of source material. Perhaps a redefinition of the characteristics of Climax-type porphyry deposits, is warranted, and a re-evaluation of the importance of a specific type of lower crustal source material for the development of a major porphyry molybdenum deposit. Alternatively, perhaps the Pine Grove deposit should not be considered a "Climax-type".

Economic potential of the Quinn Canyon Range

Considering the similarities in trace element composition, location, age of emplacement and apparent isotopic signature for the Quinn Canyon Volcanic system and the Pine Grove

system, the possibility of some form of molybdenum mineralization at depth in the Quinn Canyon Range cannot be ruled out. It is unlikely that mineralization would be "economic" because: 1) the "ore body" or pluton(s) would be found at considerable depth, due to the lack of "dissection" evident at Pine Grove and other Climax-type deposits, 2) the rhyolite samples from QC with the most "economic promise" represent only a small portion of the rhyolites sampled and 3) the trace element signature and source material of the QC rhyolites is significantly different than that of Climax and Urad-Henderson, the most prolific producers of molybdenum in the world.

The presence of fluorite, base metal vein deposits, anomalous concentrations of Mo, W, Pb, and Sn associated with rhyolite intrusives, and some rhyolite dikes being chemically similar to topaz rhyolites suggests that the Quinn Canyon Range has some potential for hosting Be, Li, U and Sn mineralization.

CONCLUSIONS

The major conclusions of this study are:

- 1) Rhyolitic hypabyssal and extrusive rocks in the Quinn Canyon Range exhibit considerable chemical variation. Most of the intrusive and flow samples collected can be placed into six groups, based on trace and to a lesser degree, major element chemistry.
- 2) Two different groups of "differentiated" high-silica rhyolites can be delineated; a more peraluminous, muscovite-bearing group, which is moderately enriched in incompatible elements and depleted in LREE, MREE, Ti, Ba, Zr, and Hf and an incompatible-element rich group having relatively high concentrations of Rb, Y, Nb, Th, and HREE and depleted in Ti, Ba, Eu, Hf and Zr. Chondrite-normalized REE patterns for this group are flat with low La/Ybw ratios.
- 3) The differences in trace element chemistry of these groups could be due to subtle differences in source material, with the muscovite-bearing rhyolites perhaps being the result of partial melting at a different crustal level or asssimilation of upper crustal pelitic rocks.

- 4) The most incompatible element-rich rhyolites are probably the result of fractional crystalization of a magma formed by small degree of partial melting.
- 5) The trace element signature of the Quinn Canyon rhyolites is considerably different than the granitic rocks which source the mineralization at Urad-Henderson and Climax. These differences are apparent in the lower enrichment in most key incompatible elements, an enrichment in HREE, and a depletion in LREE.
- 6) The rhyolite intrusives and extrusives associated with molybdenum mineralization at Pine Grove have in many respects similar trace element enrichment trends, as those seen in the most incompatible-element enriched Quinn Canyon rhyolite dikes. This is especially true of REE concentrations and ratios.
- 7) According to trace element chemistry, the most "evolved" Quinn Canyon rhyolites probably can qualify, with minor exceptions, as topaz rhyolites (Christiansen et al., 1986).
- 8) Limited Pb isotope evidence taken from published literature for the Quinn Canyon and Pine Grove area suggests a non-depleted or non-cratonized source, unlike the granulite-facies lower crustal source proposed for Climax-type granitiods of the Colorado Mineral Belt.

9) Based on similarities with the Pine Grove system in geologic setting, trace element chemistry of rhyolites, age of emplacement and to a lesser extent isotope data, the occurrence of molybdenum mineralization at depth in the Quinn Canyon Range cannot be precluded at this stage of study. It must be emphasized that the generating pluton and mineralization, if any, would have a significantly different source material, than that of the Climax-type deposits of the Colorado Mineral Belt and would likely be non-economic.

Future work

The relationship between the Quinn Canyon rhyolites, topaz rhyolites associated with high level lithophile-type metalization and the granitiods associated with porphyry Mo, W, Sn mineralization, warrants further attention. Comparisons would be greatly enhanced by a detailed Pb, and Sr isotope study of Quinn Canyon and other mineralized intrusive centers (such as Pine Grove). This type of detailed study, would help elucidate the importance of a granulite facies lower crustal source material, for producing magmas which later generate the types of metallization mentioned previously.

A exhaustive K-Ar, Pb and Sr isotope study, would be helpful in determining the genetic relationship between silicic rocks and the igneous and metallization history of the Quinn Canyon volcanic center.

APPENDIX A

APPENDIX A

Chemical Analyses

Table 4. Chemical analyses of the Quinn Canyon silicic rocks.

Group Sample	1 eQC-3A	1 QC9-1	1 QC9-2	2 QC11A	2 QC11B	2 QCJW4B	2 QC15N	2 QC-10	2 QC-9E
Wt %									
SiO,	71.06	70.54	70.13	71.04	70.63	70.76	72.60	71.14	71.22
TiO ₂	0.51	0.49	0.45	0.32	0.33	0.28	0.23	0.36	0.33
ALO,	14.65	14.88	13,96	14.15	14.26	13.80	13.65	14.18	14.15
FeO	3.36	2.80	2.74	2.63	2.75	2.60	2.01	2.77	2.35
MnO	0.06	0.05	0.04	0.05	0.05	0.06	0.04	0.04	0.04
MgO	0.97	0.53	0.36	0.30	0.45	0.55	0.40	0.42	0.42
CaO	3.13	2.44	2.58	1.37	1.45	1.51	0.96	0.97	0.98
Na _z O	2.67	2.76	2.67	2.75	2.82	1.68	2.68	2.57	3.36
ΚO	3.50	3.45	3.43	5.02	4.56	4.89	4.78	4.95	5.23
Na _s O K _s O P _s O _s	0.10	0.09	0.09	80.0	80.0	0.06	0.04	0.09	0.09
PPM									
Cu	1	0	0	0	0	0	0	0	0
Zn	62	<i>77</i>	51	62	56	65	48	64	32
Rb	138	132	170	162	158	147	155	174	216
Sr	365	367	320	248	205	119	146	184	225
Y	19	16	20	37	38	56	40	36	43
Zr	186	180	164	318	343	367	288	343	329
Nb	14	15	13	24	24	26	24	25	26
Hf	5.1	5.5	4.0	8.4	8.7	9.1	7.7	8.0	8.7
Th	14.2	14.1	14.3	19.0	18.5	19.1	19.2	18.5	19.6
Cr	11	4	4	4	5	6	7	3	3
Sc	7.2	5.4	5.1	5.8	6.6	5.8	4.4	5.8	5.6
Ba	551	806	490	1367	1270	1434	1516	1304	1095
La	33.3	29.9	30.7	64.3	75.6	81.0	75.1	62.7	57.2
Ce	69.0	65.7	67.4	134.1	140.6	138.6	134.1	122.4	124.5
Sm	6.3	5.4	5.7	9.0	9.4	10.8	10.8	8.9	10.2
Eu	1.37	1.36	1.12	2.01	1.96	2.13	1.91	1.81	1.83
Tb	0.90	0.87	0.85	1.20	1.13	1.16	1.20	1.18	1.23
Yb	1.83	1.94	1.69	3.31	3.43	3.32	3.34	3.22	2.99
Lu	0.33	0.30	0.27	0.49	0.52	0.51	0.50	0.42	0.50

Table 4 (cont.).

Group Sample	3 •QC-16	3 QC19A	3 QC-15	3 QC-8	3 QC9-5	3 QC-14	3 QC9-4	3 QC-6	3 QC-1A
Wt%									
SiO,	72.89	75.08	75.42	76.71	76.88	75.48	77.34	75.12	74.70
TIO,	0.22	0.13	0.09	0.09	0.11	0.10	0.10	0.08	0.13
ALO,	13.53	12.80	12.82	12.66	12.72	13.35	12.92	13.10	13.20
FeO	2.05	1.53	1.30	0.83	1.18	1.43	0.43	1.39	1.47
MnO	0.05	0.02	0.02	0.00	0.02	0.02	0.01	0.05	0.04
MgO	0.24	0.15	0.11	0.00	0.06	0.17	0.00	0.05	0.07
CaO	1.01	0.49	0.43	0.18	0.11	0.22	0.14	0.40	0.35
Na ₂ O	3.41	2.68	3.28	3.80	2.45	3.48	2.72	3.18	3.19
ΚŌ	4.65	5.20	5.08	4.89	5.12	4.37	5.40	5.27	5.40
P ₂ O ₅	0.05	0.01	0.01	0.01	0.03	0.01	0.01	0.01	0.02
PPM									
Cu	0	0	1	0	11	2	0	0	0
Zn	53	50	44	9	12	41	13	50	55
Rb	169	235	158	185	220	127	233	189	243
Sr	130	98	37	52	97	65	80	46	125
Y	46	49	58	48	38	51	42	63	44
Zr	276	210	244	247	167	208	160	197	214
Nb	37	23	39	38	22	33	22	48	23
Hf	7.9	6.5	7.5	8.0	5.0	6.8	5.0	7.1	6.5
Th	22.3	36.2	20.1	16.9	28.2	19.0	27.9	24.0	35.6
Cr	4	3	3	3	3	3	2	8	4
Sc	4.0	5.3	3.0	2.1	4.2	4.8	3.7	3.4	6.0
Ba	737	883	495	205	612	929	312	185	906
La	59.5	66.6	44.3	27.7	45.8	52.0	32.8	44.2	65.8
Ce	131.0	127.7	97.9	65.3	93.0	106.0	76. 1	97.6	127.2
Sm	9.4	8.8	10.8	7.6	6.5	11.7	5.5	10.5	8.7
Eu	1.07	1.32	0.82	0.56	0.79	1.33	0.31	0.29	1.22
Tb	1.22	1.62	1.32	1.03	1.32	1.26	1.27	1.43	1.56
Yb	4.05	3.61	4.46	3.58	2.93	4.52	3.25	4.07	3.03
Lu	0.60	0.55	0.67	0.60	0.49	0.64	0.51	0.69	0.51

Table 4 (con't).

Group Sampl	3 eQC-12	4 QC9-9	4 2016	4 2012	4 2015	5 2010	5 2011	5 2008	5 QC-5
Wt %									
SiO,	73.60	75.99	75.84	75.79	76.72	78.13	77.22	76.72	79.19
TIO,	0.10	0.12	0.13	0.13	0.13	0.04	0.04	0.03	0.03
ALO,	13.14	13.03	13.14	13.68	12.79	12.55	12.75	12.80	11.65
FéO	1.35	0.81	0.94	0.16	0.63	0.29	0.73	0.61	0.37
MnO	0.04	0.00	0.01	0.00	0.00	0.01	0.01	0.00	0.00
MgO	0.09	0.04	0.00	0.00	0.00	0.00	0.00	0.00	0.00
CaO	1.27	0.19	0.30	0.28	0.13	0.18	0.18	0.18	0.11
Na ₂ O	2.23	2.36	2.99	2.69	2.27	2.95	3.33	3.01	2.28
ΚĊ	5.44	5.61	5.38	5.54	5.17	4.62	4.41	4.87	4.89
P ₂ O ₅	0.00	0.01	0.02	0.01	0.00	0.01	0.01	0.01	0.00
PPM									
Cu	0	0	0	0	0	0	0	0	0
Zn	25	15	19	11	9	7	7	7	5
Rb	205	233	224	242	224	282	213	299	297
Sr	65	102	118	134	94	31	45	27	29
Y	61	30	37	28	25	43	47	48	46
Zr	258	175	228	220	230	91	108	101	93
Nb	37	21	22	23	24	19	24	25	23
Hf	8.3	5.2	6.5	6.4	6.9	3.9	4.1	4.1	3.8
Th	20.3	27.2	34.1	22.8	20.5	25.2	33.5	21.2	15.1
Cr	13	2	1	2	4	1	1	1	3
Sc	3.2	4.5	4.8	5.4	5.5	2.8	3.0	3.1	2.9
Ba	711	717	996	1008	990	44	73	46	146
La	54.6	30.0	18.7	23.1	10.3	4.7	12.9	5.1	2.9
Ce	111.4	34.7	22.4	58.9	16.6	4.8	36.4	7.1	6.9
Sm	11.4	3.9	3.7	4.6	2.1	1.6	4.8	2.0	1.6
Eu	1.10	0.52	0.54	0.59	0.23	0.02	0.11	0.03	0.16
Tb	1.30	1.17	1.40	1.08	0.93	1.13	1.48	1.03	0.92
Yb	4.46	2.74	2.13	2.18	2.66	3.55	3.89	3.39	2.94
Lu	0.68	0.47	0.44	0.43	0.40	0.53	0.60	0.53	0.48

Table 4 (con't).

Group Sample	5 2007	5 2022	6 QC-19C	6 QC-20	6 QC9-3	6 QC-13	6 QC-19
Wt %							
SiO ₂	80.01	77.35	75.83	78.30	75.66	75.83	78.94
TiO,	0.03	0.09	0.05	0.03	0.05	0.04	0.04
ALO,	11.28	12.55	12.13	12.79	12.37	12.20	11.69
FeO	0.31	0.87	1.04	0.33	1.11	0.68	0.80
MnO	0.00	0.01	0.02	0.01	0.03	0.01	0.06
MgO	0.03	0.01	0.20	0.03	0.20	0.62	0.02
CaO	0.20	0.28	0.89	0.16	1.28	1.44	0.28
Na ₂ O	2.06	2.30	2.74	2.93	2.20	0.14	3.38
ΚŌ	4.43	4.83	4.62	4.91	4.92	4.78	4.30
P ₂ O ₅	0.02	0.02	0.00	0.01	0.00	0.00	0.01
PPM							
Cu	0	0	0	0	0	0	0
Zn	5	70	53	11	50	45	45
Rb	270	205	285	399	301	325	541
Sr	30	64	13	19	17	20	22
Y	44	27	114	70	118	109	173
Zr	78	153	179	111	177	188	130
Nb	24	24	73	29	72	87	98
Hf	4.0	4.7	8.3	4.6	8.0	9.1	7.5
Th	12.7	25.5	30.8	24.9	30.0	36.2	51.3
Cr	2	1	0	8	5	4	1
Sc	2.7	3.9	1.6	3.0	2.0	1.0	2.7
Ba	109	360	115	149	148	263	168
La	3.6	8.0	15.6	6.7	19.7	32.8	14.7
Ce	5.6	13.4	40.2	16.8	39.3	27.7	45.6
Sm	1.6	1.7	12.8	5.2	13.5	12.1	11.5
Eu	0.09	0.08	0.19	0.09	80.0	0.35	0.04
Tb	0.83	1.04	1.84	1.22	1.97	2.08	2.44
Yb	2.94	2.49	5.69	4.41	6.12	6.90	8.68
Lu	0.51	0.41	1.12	0.74	1.00	1.05	1.58

Table 5. Chemical analyses of fluorite, highly altered samples and other samples from Quinn Canyon.

	Fluorite									
Samp	leQC-17	QC-9B	QC-9C	1107	1001	1102b	1109	QJW2A	QJW2B	QJW2C
110 oz										
Wt %			70.05		3 0.40			50.40		7 0.00
SiO ₂	_	71.16	72.05	76.50	76.16	81.34	79.71	76.40	74.98	73.93
TiO,	_	0.33	0.33	0.25	0.17	0.04	0.18	0.10	0.12	0.11
ALO,	_	14.21	14.36	12.47	12.58	11.43	10.89	13.01	12.71	13.37
FeO	-	2.55	2.49	1.40	0.26	0.73	0.84	0.23	1.53	1.33
MnO	_	0.05	0.05	0.03	0.01	0.00	0.01	0.01	0.03	0.01
MgO	-	0.44	0.32	0.21	0.00	0.00	0.00	0.63	0.16	1.63
CaO	_	1.29	0.49	0.28	0.22	0.08	0.17	0.23	1.04	0.37
Na ₂ O K ₂ O	-	3.03	2.76	0.05	2.61	0.07	2.08	0.16	0.07	0.30
Κ ₂ Ο	-	5.04	5.47	4.79	5.24	2.87	4.09	6.60	5.88	5.56
P ₂ O ₅	_	0.08	0.09	0.05	0.01	0.01	0.03	0.01	0.01	0.00
PPM										
Cu	3	0	0	0	0	0	0	0	0	0
Zn	2	40	61	43	15	26	17	16	78	73
Rb	8	196	226	209	286	133	148	237	196	159
Sr	1184	253	210	83	105	38	166	11	14	15
Y	0	40	38	17	18	100	20	56	53	54
Zr	75	339	337	253	150	188	238	264	271	278
Nb	0	25	26	16	23	84	16	37	34	36
Hf	0.4	8.9	8.5	7.0	3.8	9.0	5.6	8.2	7.8	8.4
Th	0.1	20.6	20.4	23.9	27.6	34.0	13.5	15.8	18.3	20.7
Cr	1	3	4	5	1	3	3	3	2	1
Sc	0.6	5.4	5.5	3.3	2.7	0.6	2.8	3.2	5.2	3.9
Ba	10	1180	1120	1640	215	326	1710	1110	1111	1113
La	1.3	55.1	54.5	55.1	100	40	20.0	45 4	E0 0	27.0
					12.8	4.3	30.9	15.1	58.3	37.8
Ce	2.1	128.6	118.3	97.8	28.3	15.9	59.5	42.3	130.7	84.1
Sm	0.5	10.2	9.8	4.7	2.3	10.9	5.5	3.8	11.3	8.4
Eu	0.04	1.71	1.75	1.06	0.26	0.04	0.79	0.48	1.34	0.94
Tb	0.31	1.18	1.08	1.04	1.11	1.89	0.79	0.71	1.23	1.21
Yb	0.38	3.30	2.58	1.65	1.18	6.55	2.53	4.00	4.01	4.64
Lu	0.05	0.48	0.44	0.32	0.22	1.09	0.33	0.58	0.59	0.69

Table 6. Commercial analyses by Bondar and Clegg, Ltd.

Sample	Qc9-3	Qc-13	Qc-19	Qc-19c	Qc-20
PPM					
Pb	26	17	11	21	17
Мо	1	1	3	1	2
Sn	<.5	<.5	15	7	10
Ag	<.5	.5	.8	<.5	<.5

Table 7. Chemical analyses of rhyolites from Mt. Emmons, Urad-Henderson and Pine Grove.

				Urad	Henderso				Mt. Emmons	F	Pine Grov	e]
	1						На	nderson	1	·		١
0	Primos	Primos	Urad	Urad	Urad	Urad			-	DC 0	DO F	DC 4
Sempi	eH4094	H4315	H4225	8077	UUOS	UUPCX	A7RMC	RMPS1	ME111	PG-3	PG-5	PG-6
Wt %												
SiO,	76.19	72.61	78.35	77.11	79.72	76.42	77.62	75.55	75.9 9	78.93	75.48	76.15
TIO,	0.12	0.06	0.12	0.11	0.13	0.16	0.13	0.13	0.23	0.02	0.03	0.02
AĻŌ,	12.60	12.76	11.94	13.26	11.86	12.70	12.10	12.40	12.51	11.39	12.74	13.48
FeO	0.85	0.28	0.49	0.32	1.02	0.92	0.57	1.34	1.35	0.53	0.78	0.67
MnO	0.20	0.10	0.02	0.13	0.42	0.05	0.05	2.20	0.07	0.02	0.05	0.06
MgO	0.68	0.03	0.11	0.03	0.12	0.05	0.04	0.14	0.29	0.04	0.29	0.17
CaO	0.55	3.07	0.66	0.33	0.35	0.42	0.70	0.57	0.70	0.44	0.89	0.23
Na,O	2.78	0.95	2.24	0.28	0.12	0.29	1.93	0.18	2.68	0.66	3.27	0.95
K,Ō	5.53	8.81	5.65	6.40	4.61	5.65	5.54	4.55	5.25	8.16	4.24	5.37
Na _s O K _s O P _s O _s	0.01	0.01	0.01	0.00	0.01	0.02	0.01	0.02	0.04	0.01	0.01	0.01
PPM												
Cu	6	8	8	11	9	7	9	14	12	18	0	0
Zn	101	30	10	51	278	13	8	508	60	16	56	42
Rb	450	859	584	638	487	476	483	459	321	348	425	507
Sr	6	4	15	4	14	9	36	23	19	21	22	7
Y	49	177	67	67	77	62	63	73	36	70	90	118
Zr	101	79	106	96	115	148	127	118	209	73	74	78
Nb	83	98	81	113	86	86	94	86	80	35	46	57
Hf	5.3	4.9	4.9	3.5	4.2	6.4	4.8	4.0	7.9	1.2	3.2	4.2
Th	55.9	25.7	61.7	51.7	57.2	72.5	62.9	59.0	71.2	20.4	22.2	24.0
Sc	-	_	-	-	-	_	_	_	_	_	_	-
Ba	88	74	92	97	101	121	150	148	100	106	112	114
La .	49.7	36.1	51.3	42.1	48.1	64.6	42.4	45.9	58.1	12.5	11.8	13.8
Ce	71.1	48.6	83.2	59.4	78.6	106.1	68.1	81.1	81.3	19.4	29.8	34.9
Sm	6.7	5.4	7.4	6.5	8.6	7.6	7.0	7.2	9.4	7.1	8.3	9.0
Eu	0.26	0.14	0.29	0.18	0.32	0.38	0.29	0.28	0.36	0.10	0.41	0.61
Ъ	1.97	1.21	2.16	1.82	2.20	2.55	2.26	2.18	2.45	1.27	1.32	1.43
Υb	4.70	7.21	3.80	3.53	5.04	3.84	3.97	3.92	3.33	4.61	3.59	4.07
LJ.	0.83	1.44	0.74	0.62	0.87	0.65	0.69	0.66	0.63	0.75	0.58	0.73

Table 7 (con't).

	Pine	Grove (Keith, 19	982)*
	Phase Five Porphyry	Pine Grove Porphyry	Phase Four Porphyry
Sample	152	142	155
Wt %			
SiO,	75.83	75.13	74.90
TIO,	0.03	0.04	0.04
ALO,	11.67	12.98	12.23
Fe,O,	0.67	1.02	0.67
MnO	0.03	0.12	0.05
MgO	0.17	0.02	0.41
CaO	0.96	0.85	1.14
Na _s O	1.02	2.75	1.12
K,Ô	7.47	5.76	7.08
P,O,	0.02	0.01	0.02
PPM			
Cu	_	_	_
Zn	47	84	69
Rb	329	412	349
Sr	39	34	33
Y	62	68	78
Zr	83	86	99
Nb	41	34	37
Hf	3.7	3.5	3.4
Th	25.5	27.8	27.4
Cr	_	_	-
Sc	7.8	9.7	7.8
Ba	100	120	120
La	15.5	16.4	15.8
Ce	38.4	43.2	41.9
Sm	8.2	8.8	8.5
Eu	0.10	0.07	0.06
Тъ	1.68	1.93	1.70
Yb	6.00	6.60	7.00
Lu	0.83	1.02	0.95

^{*} analyses from Keith (1982. Some trace element values represent the arthimetic mean of replicate analyses.



APPENDIX B

Analytical Methods

Representative 1kg. samples were trimmed to remove weathered rinds, ground to a fine powder (200 mesh), and dried in an evacuated oven at 100c for 24 hours to remove excess water.

Major element oxide percentages were determined by XRF using fused glass wafers. Glass wafers were made by homogenizing 1.00000 grams of sample, 9.00000 grams of lithium tetraborate, and .1600 grams of ammonium nitrate, in a platinum-gold alloy crucible. This mixture was continuously agitated while being heated at 1100 C for 20 minutes. The resultant liquid was poured into a heated Pt-Au mold and slowly cooled to room temperature.

The trace elements Rb, Sr, Nb, Y, Cr, Ni, Cu, Zn, Zr, and Y were also analyzed by XRF, using pressed powder pellets, with a sample/celluolose "amercil" binder ration of 4:1.

La, Ce, Sm, Eu, Tb, Yb, Lu, Th, Hf, Sc and Cr were analyzed by INAA (Instrumental Neutron Activication Analysis). 1.00000 gram samples were sealed in polyvinyl vials and irradiated for 18 hours over a 3 day period.

All analyses were performed at the Michigan State
University Department of Geological Sciences XRF and Neutron
Activation Laboratory. Analytical precision and accuracy are
given for replicate analyses of USGS standard W-2 in table 8.

Table 8. Precision and accuracy.

A. Concentration of U.S.G.S. standard G-2 determined by X-ray fluorescence (XRF)

				Reported
Wt%	n	Mean	Std. Dev.	(Govindarajo, 1984)
SiO ₂	3	69.39	.13	69.22
Al ₂ O ₃	· 3	15.41	.01	15.40
FeO	3	*2.39	.01	1.44
Fe ₂ O ₃				1.07
MgO	3	.76	.03	.75
CaO	3	1.98	.02	1.96
Na ₂ O	3	4.01	.09	4.06
K ₂ O	3	4.48	.01	4.46
TiO ₂	3	.48	.00	.48
P ₂ O ₅	3	.13	.00	.13
MnO	3	.03	.00	.03

B. Concentration of U.S.G.S. standard G-2 determined by X-ray fluorescence (XRF).

				Reported
PPM	n	Mean	Std. Dev.	(Govindarajo, 1984)
Cu	3	11	2.52	10
Zn	3	93	.58	84
Rb	3	172	1.53	170
Sr	3	481	2.08	480
Y	3	8	.58	11
Zr	3	296	2.00	300
Nb	3	13	1.16	13
Ва	3	1921	68.40	1900

C. Concentration of U.S.G.S. standard W-2 determined by instrumental neutron activation analysis (INAA).

				Reported
PPM	n	Mean	Std. Dev.	(Govindarajo, 1984)
La	4	11.7	1.61	10.4
Ce	4	22.7	.69	23
Sm	4	3.3	.15	3.3
Eu	4	1.12	.04	1.1
Tb	4	.77	.42	.66
Yb	4	1.50	.09	2.1
Lu	4	.36	.02	.33
Hf	4	2.7	.17	2.6
Th	4	2.2	.15	2.4
Cr	4	88	3.71	92

^{*} Fe reported as FeO.



APPENDIX C

Location of Samples

Sample		Location					
QC-1A		SW	Sec	4	R56E	T2N	
QC-3A		SW	Sec	4	R56E	T2N	
QC-5		SW	Sec	4	R56E	T2N	
QC-6		SW	Sec	4	R56E	T2N	
QC-8	NE	SE	Sec	10	R56E	T3N	
QC-9B,C,E	NE	SE	Sec	10	R56E	T3N	
QC-10	NW	SE	Sec	10	R56E	T3N	
QC-11A,B	NW	SE	Sec	10	R56E	T3N	
QC-12	NW	SE	Sec	10	R56E	T3N	
QC-13	SE	NE	Sec	15	R56E	T3N	
QC-14	SE	NE	Sec	15	R56E	T3N	
QC-15	SE	NW	Sec	15	R56E	T3N	
QC-15N	SE	NW	Sec	15	R56E	T3N	
QC-16	SE	NE	Sec	16	R56E	T3N	
QC-17	NE	NE	Sec	16	R56E	T3N	
QC-19	NW	SW	Sec	21	R57E	T3N	
QC-19A, C	SE	NW	Sec	15	R56E	T3N	
QC-20	SW	SE	Sec	15	R57E	T3N	
QCJW2A, JW2B, JW2C	NW	SW	Sec	3	R57E	T3N	
QCJW4B	SW	NE	Sec	4	R57E	T3N	
QC9-1	NW	NM		4	R56E	T3N	
QC9-2	NW	NW	Sec	4	R56E	T3N	
QC9-3	NW	NW		4	R56E	T3N	
QC9-4		NW	Sec	4	R56E	T3N	
QC9-5		NW	Sec	4	R56E	T3N	
QC9-9		NW	Sec		R56E	T3N	
2007			Sec		R56E	T3N	
2008			Sec	4	R56E	T3N	
2010			Sec	4	R56E	T3N	
2011			Sec	4	R56E	T3N	
2012			Sec	4	R56E	T3N	
2015			Sec	4	R56E	T3N	
2016			Sec	4	R56E	T3N	
2022			Sec	4	R56E	T3N	



LIST OF REFERENCES

- Alderton, D.H.M., Pearce, J.A., and Potts, P.J., 1980, Rare earth element mobility during granite alteration: evidence from southwest England: Earth and Planetary Science Letters, vol. 49, p. 149-168.
- Allegre, C.J., Minster, J.F., 1978, Quantitative models of trace element behavior in magmatic processes: Earth and Planetary Science Letters, vol. 38, p. 1-25.
- Armstrong, R.L., Ekren, E.B., McKee, E.H., and Noble, D.C., 1969, Space-time relations of Cenozoic silicic volcanism in the Great Basin of the Western United States:

 American Journal of Science, vol. 267, p. 478-490.
- Armstrong, R.L., 1970, Geochronology of Tertiary igneous rocks, Eastern Basin and Range Province, Western Utah, Eastern Nevada, and vicinity, U.S.A.: Geochemica et Cosmochimica Acta, 1970, vol. 34, p. 203-232.
- Burt, D.H., Sheridan, M.F., Bikun, J.V. and Christiansen, E.H., 1982, Topaz rhyolites-distribution, origin, and significance for exploration: Economic Geology, vol. 77, p. 1818-1836.
- Campbell, I.H., Lesher, C.M., Coad, P., Franklin, J.M., Gorton, M.P., and Thurston, P.C., 1984, Rare earth element mobility in alteration pipes below massive Cu-Zn sulfide deposits: Chemical Geology, vol. 45, p. 181-202.
- Christiansen, E.H., Burt, D.M., Sheridan, M.F. and Wilson, R.T., 1983, The petrogenesis of topaz rhyolites from the Western United States: Contributions to Mineralogy and Petrology, vol. 83, p.16-30.
- Christiansen, E.H., Sheridan, M.F., and Burt, D.M., 1986, The geology and geochemistry of Cenozoic topaz rhyolites from the western United States: Geological Society of America Special Paper 205, 82 p.
- Christiansen, R.L., and Lipman, P.W., 1972, Cenozoic volcanism and plate tectonic evolution of the Western United States. II. Late Cenozoic: Philosophical Transactions of the Royal Society of London, vol. 271, p. 249-284.

- Doe, B.R. and Zartman, R.E., 1979, Plumbotectonics, the Phanerozoic, in Barnes (ed.), Geochemistry of Hydrothermal Ore Deposits, second edition: John Wiley and Sons: New York, p. 22-70.
- Eaton, G.P., 1984, The Miocene Great Basin of western North America as an extending back-arc region: Tectonophysics, vol. 102, p. 275-295.
- Edwards, R., and Atkinson, K., 1986, Ore Deposit Geology: Chapman and Hall, 446 p.
- Farmer, G.L., and Depaolo, D.J., 1983, Origin of Mesozoic and Tertiary granite in the western United States and implications for Pre-Mesozoic crustal structure: 1: Nd and Sr isotopic studies in the geocline of the Northern Great Basins: Journal of Geophysical Research, vol. 88, p. 3379-3401.
- Farmer, G.L. and Depaolo, D.J., 1984, Origin of Mesozoic and Tertiary granite in the western United States and Implications for Pre-Mesozoic crustal structure: 2. Nd and Sr isotopic studies of unmineralized and Cu- and Momineralized granite in the Precambrian Craton: Journal of Geophysical Research, vol. 89, p. 10141-10160.
- Floyd, P.A. and Winchster, J.A., 1978, Identification and discrimination of altered and metamorphosed volcanic rocks using immobile elements: Chemical Geology, vol. 21, p. 291-306.
- Govindaraju, K. (Ed.), 1984, Geostandards Newsletter, vol. 8, p. 1-39.
- Hildreth, W., 1979, The Bishop Tuff: evidence for the origin of compositional zonation in silicic magma chambers: Geological Society of America Special Paper 180, p. 43-75.
- Keith, J.D., 1980, Miocene porphyry intrusions, volcanism and mineralization, southwestern Utah and Eastern Nevada: M.S. thesis, University of Wisconsin, Madison, 166 p.
- Porphyry molybdenum system, southwestern Utah: Ph.d. thesis, University of Wisconsin, Madison, 246 p.
- Keith, J.D., Shanks, W.C., Archibald, D.A., and Farrar, E., 1986, Volcanic and intrusive history of the Pine Grove porphyry molybdenum system, southwestern Utah: Economic Geology, vol. 81, p. 553-577.

- Kral, V.E., 1951, Mineral Resources of Nye County, Nevada: Nevada University of Geology and Mining, no. 50, 223 p.
- Lamarre, A.L. and Hodder, R.W., 1978, Distribution and genesis of fluorite deposits in the western United States and their significance to metallogeny: Geology, vol. 6, p. 236-238.
- Lindsey, D.A., 1982, Tertiary volcanic rocks and uranium in the Thomas Range and northern Drum Mountains, Juab Co., Utah: United States Geological Survey Professional Paper 1221, 71 p.
- Lipman, P.W., Prostka and Christiansen, R.L., 1972. Cenozoic volcanism and plate-tectonic evolution of the Western United States. I. Early and Middle Cenozoic: Philosophical Transactions of the Royal Society of London, vol. 271, p. 217-248.
- Lipman, P.W., Fisher, F.S., Mehnert, H.H., Naeser, C.W., Luedke, R.G., and Steven, T.A., 1976, Multiple ages of Mid-Tertiary mineralization and alteration in the western San Juan Mountains, Colorado: Economic Geology, vol. 71, p. 71-588.
- Maclean, W.H., and Kranidiotis, P., 1987, immobile elements as monitors of mass transfer in hydrothermal alteration: Phelps Dodge massive sulfide deposit, Matagami, Quebec: Economic Geology, vol. 82, p. 951-962.
- Minster, J.F., and Allegre, 1978, Systematic use of trace elements in igneous processes Part III: Inverse problem of batch partial melting in volcanic suites: Contributions to Mineralogy and Petrology, vol. 68, p. 37-52.
- Mutschler, F.E., Wright, E.G., Ludington, S. and Abbott, J.T., 1981, Granite-molybdenite systems: Economic Geology, vol. 76, p. 870-893.
- Palacios, C.M., Hein, U.F., and Dulski, P., 1986, Behavior of rare earth elements during hydrothermal alteration at the Buene Esperanza copper-silver deposit, northern Chile: Earth and Planetary Science Letters, v. 80, p. 208-216.
- Pearce, J.A., Harris, N.B.W., and Tindle, A.G., 1984, Trace element discrimination diagrams for the tectonic interpretation of granitic rocks: Journal of Petrology, vol. 25, part 4, p. 946-983.
- Pettingill, H.S., Sinha, A.K., and Tatsumoto, M., 1984, Age and origin of anorthosites, charnokites, and granulites in the central Virginia Blue Ridge: Nd and Sr isotopic evidence: Contributions to Mineralogy and Petrology vol. 85, p. 279-291.

- Rowley, P.D., Lipman, P.W., Mehnert, H.H., Lindsey, D.A., and Anderson, J.J., 1978, Blue Ribbon Lineament, an east-trending structural zone within the Pioche Mineral Belt of southwestern Utah and eastern Nevada: United States Geological Survey Journal of Research, vol. 6, p. 75-192.
- Sainsbury, C.L., and Kleinhampl, F.J., 1969, Fluorite deposits of the Quinn Canyon Range, Nevada: United States Geological Survey Bulletin 1272-C, p. C1-C22.
- Stacey, J.S., Zartman, R.E., and Nkomo, I.T., 1968, A lead isotope study of galenas and selected feldspars from mining districts in Utah: Economic Geology, vol. 63, p. 796-814.
- Stein, H.J., 1985, A lead, strontium, and sulfur isotope study of Laramide-Tertiary intrusions and mineralization in the Colorado Mineral Belt with emphasis on Climax-type porphyry molybdenum deposits plus a summary of other newly acquired isotopic and rare earth element data: Ph.d. thesis, University of North Carolina at Chapel Hill, 493 p.
- Stewart, J.H., and Carlson, J.E., 1977, Geologic map of Nevada: Nevada Bureau of Mines and Geology.
- Stewart, J.H., Moore, W.J. and Zietz, I., 1977, East-west patterns of Cenozoic igneous rocks, aeromagnetic anomalies and, mineral deposits, Nevada.
- Tweto, O. and Sims, P.K., 1963, Precambrian ancestory of the Colorado Mineral Belt: Geological Society of America Bulletin, vol. 74, p. 991-1014.
- Van Alstine, R.E., 1976, Continental rifts and lineaments associated with major fluorspar districts: Economic Geology, v. 71, p. 977-987.
- Wallace, S.R., Muncaster, N.K., Jonson, D.C., Mackenzie, W.R., Bookstrom, A.A., and Surface, V.E., 1968, Multiple intrusion and mineralization at Climax, Colorado, in Ridge, J.D. ed., Ore Deposits of the United States 1933-1967 (Graton-Sales vol. 1): New York, Am Inst. Mining Metall. Petroleum Engineers, p. 605-641.
- Wallace, S.R., Mackenzie, W.B., Blair, R.G., and Muncaster, N.K., 1978, Geology of the Urad and Henderson molybdenite deposits, Clear Creek County, Colorado, with a section on a comparison of these deposits with those at Climax, Colorado: Economic Geology, vol. 73, p. 325-368.

- Westra, G. and Keith, S.B., 1981, Classification and genesis of stockwork molybdenum deposits: Economic Geology, vol. 76, p. 844-893.
- White, W.H., Bookstrom, A.A., Kamilli, R.J., Ganster, M.W.,] Smith, R.P., Ranta, D.W., and Steininger, R.C., 1981, Character and origin of Climax-type molybdenum deposits: Economic Geology 75th anniversary volume, p. 270-316.
- White, A.J.R., and Chappell, B.W., 1983, Granitoid types and their distribution in the Lachlan Fold Belt, southeastern Australia: Geological Society of America, memoir 159, p. 21-34.
- Winchester, J.A. and Floyd, P.A., 1977, Geochemical discrimination of different magma series and their differentiation products using immobile elements: Chemical Geology, vol. 20, p. 325-343.
- Zartman, R.E., 1974, Lead isotopic provinces in the cordillera of the Western United States and their geologic significance: Economic Geology, vol. 69, p. 792-805.